



International Agreement Report

Analysis of Inadvertent Pressurizer Spray Valve Opening Real Transient with RELAP5/MOD3.2

Prepared by

J. Blanco, L. Rebollo, E. Moralo, J. Pindado, P. Moreno

UNESA
C/ Francisco Gervas No. 3
28020 Madrid
SPAIN

**Office of Nuclear Regulatory Research
U.S. Nuclear Regulatory Commission
Washington, DC 20555-0001**

January 2001

Prepared as part of
The Agreement on Research Participation and Technical Exchange
under the International Code Application and Maintenance Program (CAMP)

**Published by
U.S. Nuclear Regulatory Commission**

AVAILABILITY OF REFERENCE MATERIALS IN NRC PUBLICATIONS

NRC Reference Material

As of November 1999, you may electronically access NUREG-series publications and other NRC records at NRC's Public Electronic Reading Room at www.nrc.gov/NRC/ADAMS/index.html.

Publicly released records include, to name a few, NUREG-series publications; *Federal Register* notices; applicant, licensee, and vendor documents and correspondence; NRC correspondence and internal memoranda; bulletins and information notices; inspection and investigative reports; licensee event reports; and Commission papers and their attachments.

NRC publications in the NUREG series, NRC regulations, and *Title 10, Energy*, in the Code of *Federal Regulations* may also be purchased from one of these two sources.

1. The Superintendent of Documents
U.S. Government Printing Office
P. O. Box 37082
Washington, DC 20402-9328
www.access.gpo.gov/su_docs
202-512-1800
2. The National Technical Information Service
Springfield, VA 22161-0002
www.ntis.gov
1-800-533-6847 or, locally, 703-805-6000

A single copy of each NRC draft report for comment is available free, to the extent of supply, upon written request as follows:

Address: Office of the Chief Information Officer,
Reproduction and Distribution
Services Section
U.S. Nuclear Regulatory Commission
Washington, DC 20555-0001

E-mail: DISTRIBUTION@nrc.gov
Facsimile: 301-415-2289

Some publications in the NUREG series that are posted at NRC's Web site address www.nrc.gov/NRC/NUREGS/indexnum.html are updated periodically and may differ from the last printed version. Although references to material found on a Web site bear the date the material was accessed, the material available on the date cited may subsequently be removed from the site.

Non-NRC Reference Material

Documents available from public and special technical libraries include all open literature items, such as books, journal articles, and transactions, *Federal Register* notices, Federal and State legislation, and congressional reports. Such documents as theses, dissertations, foreign reports and translations, and non-NRC conference proceedings may be purchased from their sponsoring organization.

Copies of industry codes and standards used in a substantive manner in the NRC regulatory process are maintained at—

The NRC Technical Library
Two White Flint North
11545 Rockville Pike
Rockville, MD 20852-2738

These standards are available in the library for reference use by the public. Codes and standards are usually copyrighted and may be purchased from the originating organization or, if they are American National Standards, from—

American National Standards Institute
11 West 42nd Street
New York, NY 10036-8002
www.ansi.org
212-642-4900

The NUREG series comprises (1) technical and administrative reports and books prepared by the staff (NUREG-XXXX) or agency contractors (NUREG/CR-XXXX), (2) proceedings of conferences (NUREG/CP-XXXX), (3) reports resulting from international agreements (NUREG/IA-XXXX), (4) brochures (NUREG/BR-XXXX), and (5) compilations of legal decisions and orders of the Commission and Atomic and Safety Licensing Boards and of Directors' decisions under Section 2.206 of NRC's regulations (NUREG-0750).

DISCLAIMER: This report was prepared under an international cooperative agreement for the exchange of technical information. Neither the U.S. Government nor any agency thereof, nor any employee, makes any warranty, expressed or implied, or assumes any legal liability or responsibility for any third party's use, or the results of such use, of any information, apparatus, product or process disclosed in this publication, or represents that its use by such third party would not infringe privately owned rights.

NUREG/IA-0194



International Agreement Report

Analysis of Inadvertent Pressurizer Spray Valve Opening Real Transient with RELAP5/MOD3.2

Prepared by

J. Blanco, L. Rebollo, E. Moralo, J. Pindado, P. Moreno

UNESA
C/ Francisco Gervas No. 3
28020 Madrid
SPAIN

Office of Nuclear Regulatory Research
U.S. Nuclear Regulatory Commission
Washington, DC 20555-0001

January 2001

Prepared as part of
The Agreement on Research Participation and Technical Exchange
under the International Code Application and Maintenance Program (CAMP)

Published by
U.S. Nuclear Regulatory Commission

**NUREG/IA-0194 has been produced
from the best available copy.**

ABSTRACT

This document presents the comparison between the simulation results and the plant measurements of an actual event that took place in Jose Cabrera Nuclear Power Plant (NPP) in August 30, 1984. The event was originated by a continuous and inadvertent opening of the pressurizer spray valve.

Jose Cabrera NPP is a 510 Mwth single loop Westinghouse PWR owned by UNION ELECTRICA FENOSA, S.A. (UNION FENOSA), a Spanish utility that participates in the Code Application and Maintenance Project (CAMP) as a member of UNIDAD ELECTRICA, S.A. (UNESA).

The simulation has been carried out with the RELAP5/MOD3.2 code, running on a Digital AlphaServer 2000 4/200 computer under DIGITAL-UNIX operating system.

The main phenomena of the transient have been calculated correctly and some conclusions about the performance of new models and correlations incorporated in the MOD3.2 version, have been obtained. Several considerations about spray modelling in RELAP5/MOD3.2 are given. Additionally, a comparison with the MOD2.5 version results has shown some improvements and shortcomings of the new version.

CONTENTS

ABSTRACT	iii
CONTENTS	v
LIST OF FIGURES.	vii
LIST OF TABLES	ix
EXECUTIVE SUMMARY	xi
NOMENCLATURE	xiii
1. INTRODUCTION	1
2. NUCLEAR STATION DESCRIPTION	3
3. TRANSIENT DESCRIPTION	7
4. PLANT MODEL AND CODE INPUT DESCRIPTION	15
5. STEADY STATE CALCULATION	19
5.1 Steady-State Results	19
5.2 Steady-State Peculiarities	20
5.2.1 Flow Regime Transitions	20
5.2.2 Pressure Losses	21
5.2.3 Steam Generator Pressure	21

6. TRANSIENT ANALYSIS	25
6.1 Sequence of Events	25
6.2 Plant Response to Control System Actuation	27
6.2.1 Turbine Control Valve	27
6.2.2 Pressurizer Pressure Control	28
6.2.3 Pressurizer Spray Valve	28
6.2.4 Pressurizer Level Control	30
6.2.5 Control Rod Motion	31
6.2.6 Steam-dump Control	32
6.2.7 Steam Generator Level Control	34
6.2.8 RCP Manual Trip	35
6.3 Run Statistics	35
7. SENSITIVITY CALCULATIONS	45
7.1 Flow Regime Transitions	45
7.2 Level Tracking Option in PZR	45
7.3 Pressurizer Pressure Response	46
7.4 Average Temperature Uncertainty	47
8. RELAP5/MOD3.2 - MOD2.5 COMPARISON	53
9. CONCLUSIONS	59
10. REFERENCES	63

LIST OF FIGURES

Figure 2.1	José Cabrera Nuclear Power Plant	6
Figure 3.1	Pressurizer Pressure (Kg/cm ² rel. narrow range)	10
Figure 3.2	Pressurizer Pressure(Kg/cm ² rel. wide range) & RCS Delta T (°C)	10
Figure 3.3	RCS Average Temperature (°C) & Programmed Avg. Temp. (°C)	11
Figure 3.4	Cold Leg Temperature (°C)	11
Figure 3.5	Pressurizer Level (% of span) & Programmed Level (% of span)	12
Figure 3.6	RCS Charging Flow (liters per minute, lpm)	12
Figure 3.7	Steam Generator Pressure (Kg/cm ² rel.) & Level (cm rel narrow range)	13
Figure 3.8	Feedwater & Steam Mass Flow Rate (Tonne/h)	13
Figure 3.9	Control Rod Position (% of withdrawal) & Insertion Limit (%)	14
Figure 3.10	Generator Power (MWe)	14
Figure 4.1	José Cabrera NPP Nodalization	18
Figure 6.1	Pressurizer Pressure	37
Figure 6.2	Pressurizer Level	37
Figure 6.3	Primary Average Temperature	37
Figure 6.4	Hot and Cold Leg (HL and CL) Temperatures	37
Figure 6.5	Steam Generator Pressure	38
Figure 6.6	Steam Generator Level (Narrow Range)	38
Figure 6.7	Main Feedwater and Steam Flows	38
Figure 6.8	Make-up and Let-down Flows	38
Figure 6.9	Pressurizer Heaters Power	39
Figure 6.10	Steam-dump, Tavg Control (0-580 s)	39
Figure 6.11	Steam-dump, Pressure Control (from 580 s)	39
Figure 6.12	Nuclear and Secondary Powers (0-520 s)	39
Figure 6.13	Nuclear and Secondary Powers	40
Figure 6.14	Primary-Secondary Temperature Difference	40
Figure 6.15	Pressurizer Spray Valve Flow	40
Figure 6.16	Primary System Flow	40
Figure 6.17	Primary System Delta T	41
Figure 6.18	Feedwater Temperature	41

Figure 6.19	Control Rod Position	41
Figure 6.20	Turbine Control Valve Opening	41
Figure 6.21	Core Reactivity Contributions	42
Figure 6.22	Vessel Head Flows	42
Figure 6.23	Vessel Temperatures	42
Figure 6.24	Steam Generator Levels (above the tube plate)	42
Figure 6.25	Flow Regime in SG Riser (Part 1)	43
Figure 6.26	Flow Regime in SG Riser (Part 2)	43
Figure 6.27	Core Average Moderator Density	43
Figure 6.28	Fuel Average Temperature	43
Figure 6.29	Pressurizer Wall Steam Generation	44
Figure 6.30	Pressurizer Volume Steam Generation	44
Figure 6.31	Pressurizer Total (Wall + Volume) Steam Generation	44
Figure 7.1	Sensitivity to smooth regime transition: SG Level	49
Figure 7.2	Sensitivity to smooth regime transition: MFW Flow	49
Figure 7.3	Sensitivity to level tracking: PZR Pressure	49
Figure 7.4	Sensitivity to level tracking: PZR steam generation (volume)	49
Figure 7.5	Sensitivity to level tracking: PZR steam generation (wall)	50
Figure 7.6	Sensitivity to PZR nodalization: PZR Pressure	50
Figure 7.7	Sensitivity to PZR nodalization: Spray Flow	50
Figure 7.8	Sensitivity to PZR nodalization: PZR steam generation (wall)	50
Figure 7.9	Sensitivity to Tavg uncertainty: PZR Pressure	51
Figure 7.10	Sensitivity to Tavg uncertainty: PZR Level	51
Figure 7.11	Sensitivity to Tavg uncertainty: Average Temperature	51
Figure 7.12	Sensitivity to Tavg uncertainty: SG Pressure	51
Figure 8.1	RELAP5 MOD3.2/MOD2.5 Comparison: PZR Pressure	56
Figure 8.2	RELAP5 MOD3.2/MOD2.5 Comparison: PZR Level	56
Figure 8.3	RELAP5 MOD3.2/MOD2.5 Comparison: Average Temperature	56
Figure 8.4	RELAP5 MOD3.2/MOD2.5 Comparison: SG Pressure	56
Figure 8.5	RELAP5 MOD3.2/MOD2.5 Comparison: SG Level	57
Figure 8.6	RELAP5 MOD3.2/MOD2.5 Comparison: SG Level (0-600s)	57
Figure 8.7	RELAP5 MOD3.2/MOD2.5 Comparison: PZR vapgen (volume)	57
Figure 8.8	RELAP5 MOD3.2/MOD2.5 Comparison: PZR vapgen (wall)	57

LIST OF TABLES

Table 5.1	Steady-state results at 96% nominal power	19
Table 5.2	Steam Generator Riser: Main Nodalization Parameters	22
Table 5.3	Steam Generator Riser: Flow Regime Related Results	23
Table 6.1	Sequence of events for the simulated transient	26
Table 8.1	MOD3.2/MOD2.5 comparison: Steady-state results	53

EXECUTIVE SUMMARY

This work shows the results of the analysis with RELAP5/MOD3.2 of an actual event that took place in Jose Cabrera Nuclear Power Plant (NPP) in August 30, 1984. The event was originated by a continuous and inadvertent opening of the pressurizer spray valve.

Jose Cabrera NPP is a 510 Mwth single loop Westinghouse PWR. A general purpose nodalization of the plant for RELAP5 has been used. This nodalization is being widely used in thermal-hydraulic applications and has given good results.

The inadvertent opening of the spray valve caused a reactor coolant system depressurization, producing a reactor trip. The reactor coolant pump was manually tripped half an hour later to stop the spray flow. Afterwards, the cooling of the primary system was due to natural circulation. The safety injection system (9.7 MPa shut-off pressure) did not introduce water into the primary circuit because the RCS pressure was stabilized at 10.0 MPa.

The main phenomena were reproduced in the simulation and the discrepancies were justified. Some shortcomings of the new flow maps, and associated drag and heat transfer correlations, incorporated in RELAP5/MOD3.2 for tube bundles have been identified. Several considerations about spray modeling in RELAP5/MOD3.2 are given, including some sensitivity studies. Additionally, a comparison with RELAP5/MOD2.5 results has shown the improvements of this new version.

NOMENCLATURE

AFWS	Auxiliary Feedwater System
ANM	Annular-Mist
BBY	Bubbly
CCFL	Countercurrent Flow
CVCS	Chemical and Volume Control System
ECCS	Emergency Core Cooling System
EFWS	Emergency Feedwater System
LOCA	Loss of Coolant Accident
MFW	Main Feedwater
NPP	Nuclear Power Plant
PZR	Pressurizer
RCP	Reactor Coolant Pump
RCS	Reactor Coolant System
RHRS	Residual Heat Removal System
RWST	Refueling Water Storage Tank
SG	Steam Generator
SLG	Slug

1. INTRODUCTION

This report has been prepared by UNIÓN FENOSA within the framework of the Code Applications and Maintenance Program (CAMP). It includes an assessment calculation of RELAP5/MOD3.2 /4/ against an actual event occurred at José Cabrera Nuclear Power Plant (NPP), a single-loop Westinghouse Pressurized Water Reactor (PWR). Additionally, some sensitivity calculations on model options, and a comparison with RELAP5/MOD2.5 /3/ results have been included.

This transient was already analyzed within the frame of the International Code Assessment and Applications Program (ICAP) /5/.

The simulated transient /2/ was initiated by an inadvertent opening of the pressurizer spray valve while the plant was operating at 96% of its nominal power. The consequence of this inadvertent opening was a continuous decrease of the pressurizer pressure. This decrease was intended to be stopped by reducing the turbine load, which finally did not avoid the reactor trip by for reaching the low pressurizer pressure setpoint. After the reactor trip, it was also reached the safety injection (SI) starting setpoint, but the safety injection pumps did not introduce water because the primary system pressure was always over the pumps shut-off pressure. The pressure decrease after the reactor trip was initially moderated by switching the steam-dump system to pressure mode, to increase the primary circuit average temperature. That action was supplemented by manually starting a second charging pump, to increase the pressurizer level. Those actions were not enough to stop the pressure decrease, so the reactor coolant pump (RCP) was manually stopped, avoiding in this way the water flow through the spray valve. From that moment on, the primary circuit began a phase of natural circulation cooling, with the pressure being recovered by the pressurizer heaters.

RELAP5/MOD3.2 code is implemented in a Digital AlphaServer 2000 4/200 computer under DIGITAL UNIX operating system, where all the calculations have been carried out.

José Cabrera NPP, where the transient took place, is described in Section 2, and the transient itself in Section 3. The model of the plant and RELAP5/MOD3.2 input deck

are briefly introduced in Section 4. The steady state results are explained in Section 5. Section 6 includes a detailed analysis of the results and their comparison with available plant data. Section 7 contains some interesting sensitivity calculations on model options. Section 8 includes a comparison of RELAP5/MOD3.2 with RELAP5/MOD2.5 results. Section 9 contains data on computer performance, and, finally, the main conclusions obtained are summarized in Section 10.

2. NUCLEAR STATION DESCRIPTION

Jose Cabrera NPP (Figure 2.1) is a Westinghouse PWR commercial plant, sited in Zorita de los Canes (Guadalajara), owned by UNION FENOSA, a Spanish utility /1/. The plant reached its first criticality in 1968 and was the first nuclear station connected to the Spanish electrical grid.

The Reactor Coolant System (RCS) has only one loop that includes a cold leg, reactor pressure vessel, hot leg, pressurizer, steam generator tubes, cross-over leg, and reactor coolant pump. The Chemical and Volume Control System (CVCS) and the Residual Heat Removal System (RHRS) are also connected to the reactor coolant loop.

A nominal reactor power of 510 Mwt_h is generated by the reactor core, which has a design of 69 fuel assemblies (14×14) with 2.40 m of active length. The fuel has an average enrichment of 3.60% in U-235. There are two control rod banks (A and B) and two scram banks. The nominal electrical power is 160 MWe with a frequency of 50 Hz.

The Emergency Core Cooling System (ECCS) is connected to the downcomer of the reactor vessel. This system includes one accumulator, two intermediate pressure safety injection pumps, two recirculation pumps and a jet pump. The SI pumps take borated water from the Refueling Water Storage Tank (RWST). In the recirculation phase of a Loss of Coolant Accident (LOCA), the low pressure pumps feed the SI pumps taking water from the containment sump.

The single steam generator, which thermally links the primary and secondary systems, includes a downcomer annulus, riser boiling chamber, separators and dryers.

The secondary side contains typical components: two 50% main feedwater pumps, steam line, safety (4) and steam-dump (3) valves, main steam isolation valve, turbine trip valves (2), main steam control valves (4), high (1) and low (1) pressure turbines, a condenser, heaters (4), etc.

The main feedwater is connected to the upper part of the downcomer by a feeding ring, without passing through any preheater section inside the steam generator. The

feedwater is previously heated by preheaters installed between the condenser and the steam generator. The circulation ratio (downcomer flow/feedwater flow) in the secondary side of the steam generator is 1.96 at full power.

The SG auxiliary and emergency feedwater systems (AFWS and EFWS) include one turbine driven and two motor-operated pumps. Both subsystems take cold demineralized water from a tank and start their operation automatically. The turbine-driven subsystem (EFWS) only injects water into the upper part of the downcomer after a manual action from the turbine operator, who opens an isolation valve from the Control Room. The motor-operated subsystem (AFWS) injects water automatically into the lower part of the SG tubes without operator intervention. Manual line up of this last subsystem with the upper part of the downcomer is also a possibility.

The plant operates normally in automatic mode with a constant demanded turbine power. The measured turbine power is a function of the pressure in the impulse chamber, which depends on the steam flow. The error between measured and demanded turbine power drives the turbine control valve position.

The reactor control system maintains the programmed coolant average temperature, which depends on the measured turbine power, by acting on the control bank B position. Average temperature is calculated by a combination of three thermocouples measurements in hot leg and three in the cross-over leg. This fact produces some thermal streaming effect, due to the turbulent mixing of the core outlet temperature distribution in the hot leg and due to the different cooling lengths inside the steam generator tubes in the cross-over length.

The RCS pressure is controlled by the pressurizer pressure control system, which acts on the PORV's, spray valve and heaters. The pressurizer level control system follows a level program, which depends on the RCS average temperature, by acting on the speed of one of two positive displacement charging pumps in the automatic control mode. The second charging pump is operated manually if necessary. A usual operation practice for pressurizer level recovering after reactor trip is operating with the first charging pump in automatic control and the second one in manual at full speed.

The steam generator level control system follows a constant level program, actuating

on the feedwater control valve. The error signal is based on a combination of level deviation and feedwater-steam flow mismatch.

Finally, the steam-dump system (two valves to the environment and one to the condenser) controls the primary average temperature after a turbine trip. This system can also work under secondary pressure control by following a manually selected steam generator pressure setpoint.

The safety of the plant is guaranteed by the Reactor Protection System and the Emergency Safety System.

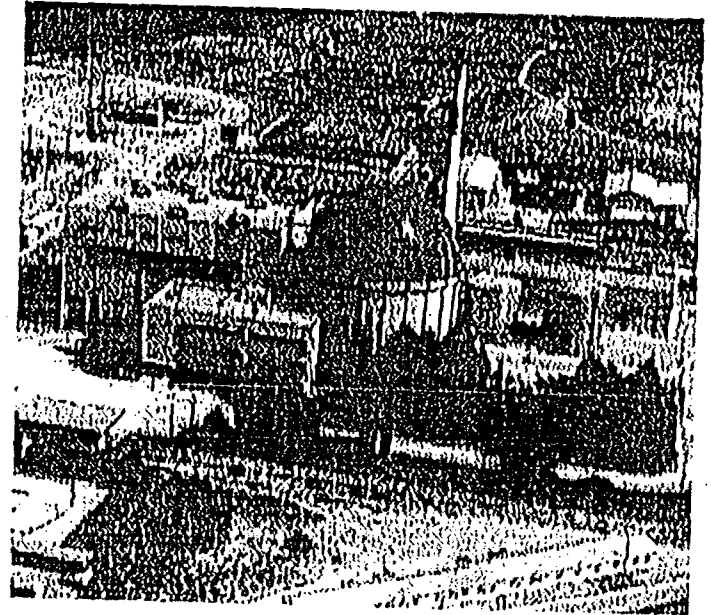
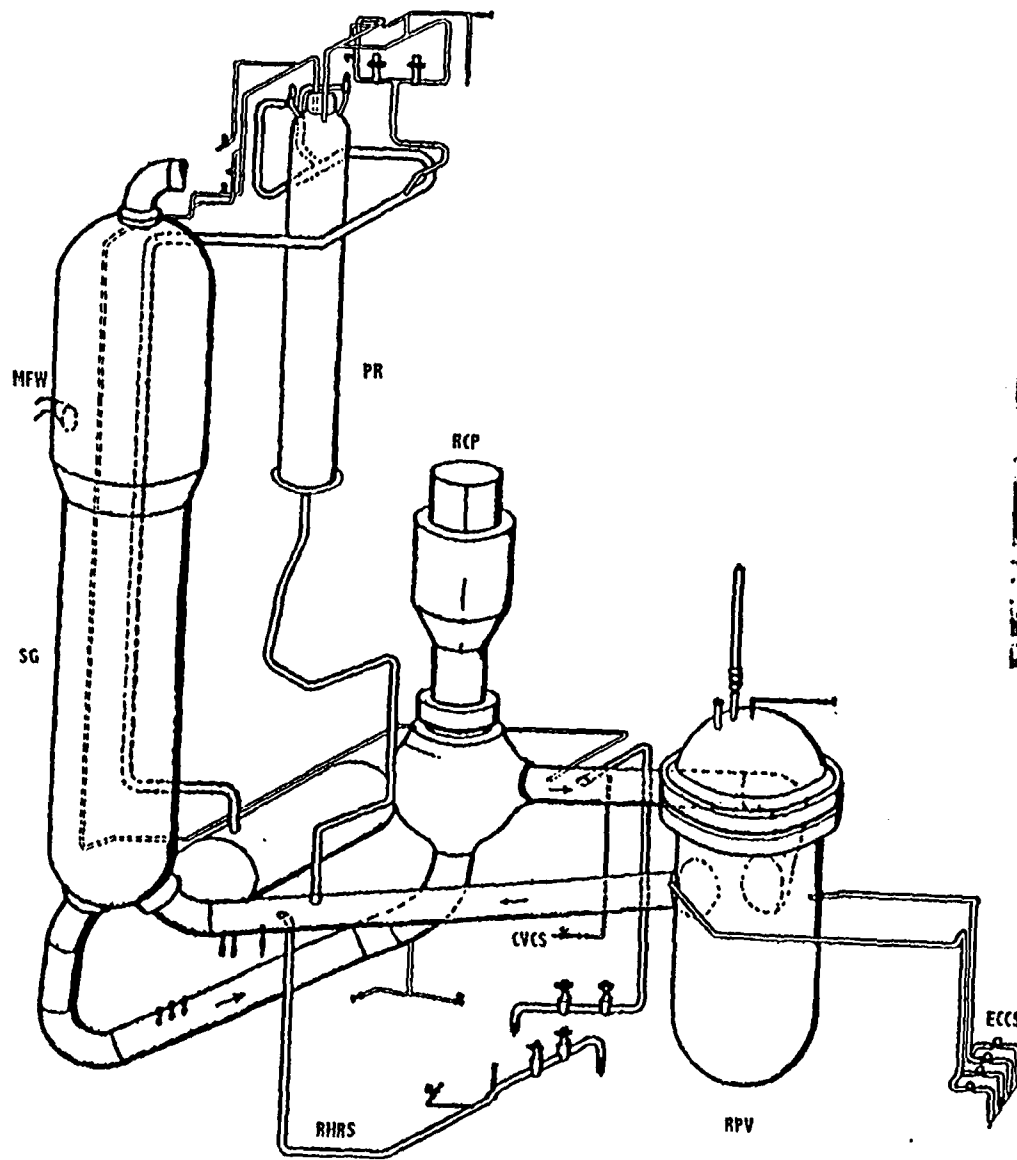


Figure 2.1. José Cabrera Nuclear Power Plant

3. TRANSIENT DESCRIPTION

The selected transient is a reactor trip occurred at José Cabrera NPP, which happened at 13:40 h, August 30, 1984 /2/. It was the 84th day of 251 nominal days at effective full power operation predicted for that cycle. The incident was initiated by a continuous and inadvertent opening of the pressurizer spray valve (PCV-400A), which remained stuck open during almost half an hour. Until the beginning of the transient, the plant had been operating at 96% thermal power under automatic control, with all the main parameters within their normal ranges.

The valve opening fault was not due to a failure of the pressurizer pressure control system, but to a failure in its driving mechanism. At that time, the only indication available in the Control Room was the demanded position of the valve. Therefore, the indicated value was 0% opening during the depressurization transient, preventing a correct diagnosis of the event. After the transient, the evaluation carried out by the NPP technical support center resulted in the installation of a valve stem actual position indicator in the Control Room. This solution was considered acceptable by the Consejo de Seguridad Nuclear (Spanish Nuclear Regulatory Commission).

Following the spray valve inadvertent opening, the primary pressure began to decrease, which was announced by the corresponding low pressure alarm. The turbine operator tried to control this decrease by means of a manual turbine load reduction. Then the pressurizer relief and spray valve indicators were checked, showing 0% demanded opening. About one minute later the isolation valves of the relief lines were closed as a preventive action.

In spite of the load reduction, the RCS pressure went on decreasing, finally reaching the reactor trip low pressure setpoint. The reactor trip induced the associated and simultaneous turbine trip. After this, the nuclear power reduction, together with the steam release through the steam-dump valves, caused a fast cooling of the primary circuit.

Because of the low pressure reached just before the reactor trip, the primary pressure decrease after the trip reached the safety injection starting setpoint (120 kg/cm² rel). The pumps did not introduce water into the primary system because the RCS pressure

was always over the pumps shut-off pressure (95.9 kg/cm² rel). The ECCS flow indicator confirmed this fact, showing 0 m³/h during the whole transient.

Just after the trip, two independent manual actions moderated the pressure decrease. First, the steam-dump system was switched from temperature to pressure control mode, to increase the primary average temperature over the no-load reference (275°C), which was accomplished by manually rising the reference pressure. Second, the extra charging pump began to introduce water in the primary system at its maximum flow, to increase the pressurizer level. This second charging pump was manually started some time before the trip, but the increasing pressurizer level did not make necessary to introduce more water than that delivered by the automatically controlled charging pump.

Additionally, the operator ordered to close the MFW isolation valve along with stopping one (of two) feedwater pump. Then the steam generator level was controlled manually with the bypass valve. This action is usually taken after any reactor trip to avoid excessive cooling.

Those actions were not enough to stop the pressure decrease. So, after a complete verification of normal conditions in the containment building, an auxiliary operator came into it. He confirmed that the spray valve was actually open.

Due to the mechanical nature of the failure, it was not possible to close the spray valve from the Control Room, and first attempts to close it locally were not successful. It was decided to trip the RCP to finish the depressurization, since this action ended the spray flow. From that moment on, the primary circuit began a phase of natural circulation cooling, and the pressurizer heaters recovered the RCS pressure.

That action, made around half an hour from the beginning of the transient, just prevented the ECCS injection. Some time later, an auxiliary operator could locally close that valve.

Throughout the incident, the operation team supervised the core behaviour by reading the core exit thermocouples temperatures to monitor the subcooling margin, which was always higher than 20°C.

The minimum measured levels were 25% for the pressurizer and -80 cm rel. for the steam generator.

About 40 minutes after the RCS depressurization was initiated, the event was already solved and the pressure being recovered with natural circulation in the RCS. The fan coolers of the vessel head were operating, without any pressurizer level symptom of a steam bubble generation in the vessel head.

At that time it was not available a process computer, which prevented knowing exactly the sequence of events and the precise chronology of the operators' intervention. Both had to be deduced from several records and graphics available in the trip report, within the limits associated with their scales, speeds and accuracy. The knowledge of systems response and operation practice had played a major role as well. In spite of these difficulties, this transient was selected as an assessment case because of its time duration and the amplitude of the variation of the main thermal-hydraulic plant variables.

Figures 3.1 to 3.10 show the available plant records, on which this validation study is based. More information about this incident can be found in /2/.

In Figure 6.1 it is shown the complete sequence, with temporal details.

For convenience, it has been chosen to keep the actual plant variable units for better comparison with the records.

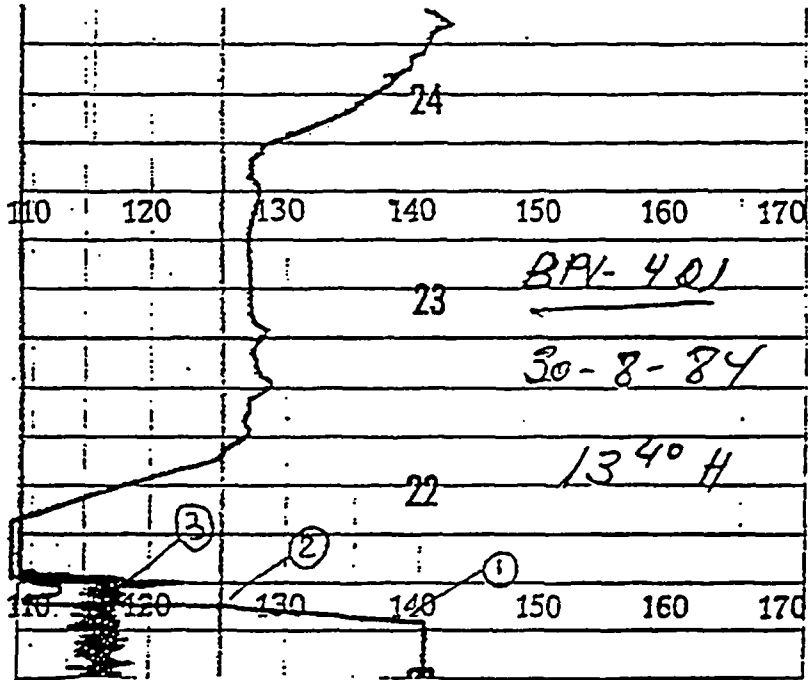


Figure 3.1. Pressurizer Pressure (Kg/cm² rel. narrow range).

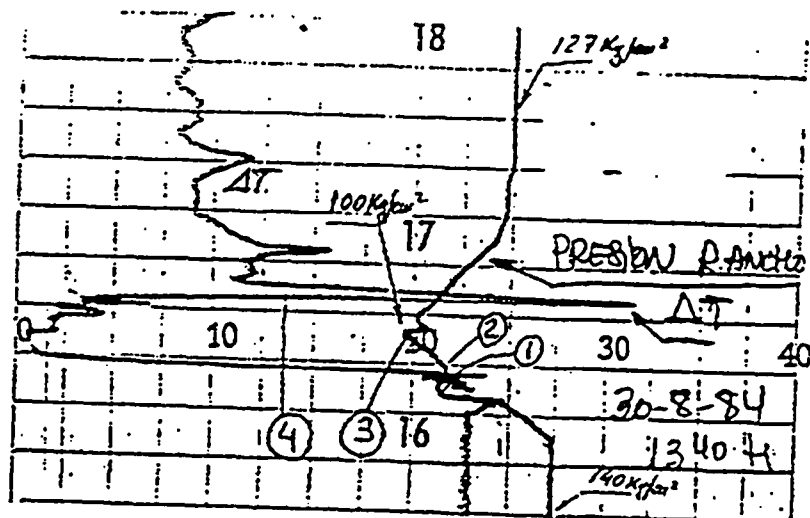


Figure 3.2. Pressurizer Pressure (Kg/cm² rel. wide range) & RCS Delta T (°C).

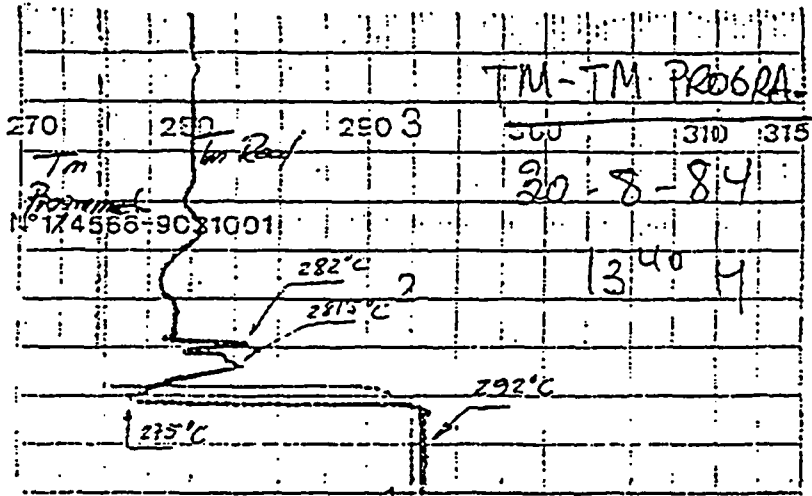


Figure 3.3. RCS Average Temperature (°C) & Programmed Avg. Temp. (°C).

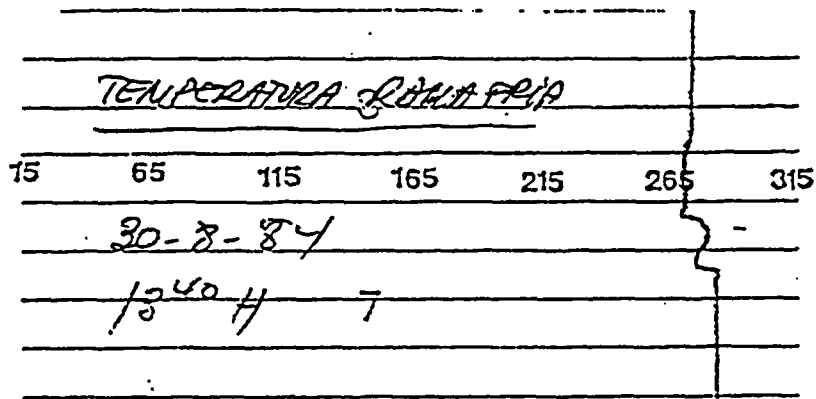


Figure 3.4. Cold Leg Temperature (°C).

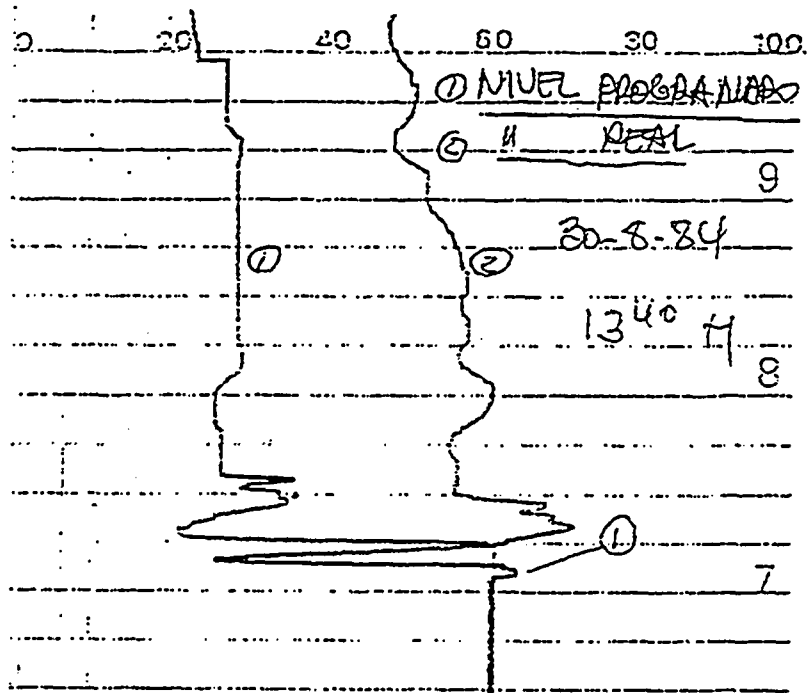


Figure 3.5. Pressurizer Level (% of span) & Programmed Level (% of span).

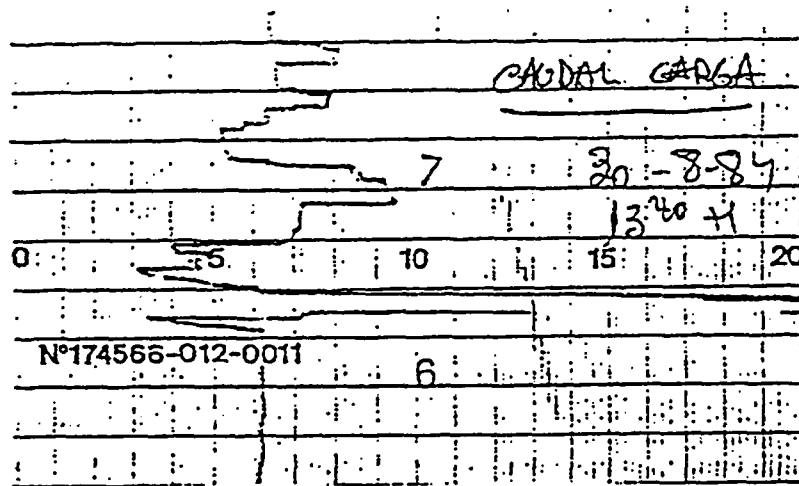


Figure 3.6. RCS Charging Flow (liters per minute, lpm).

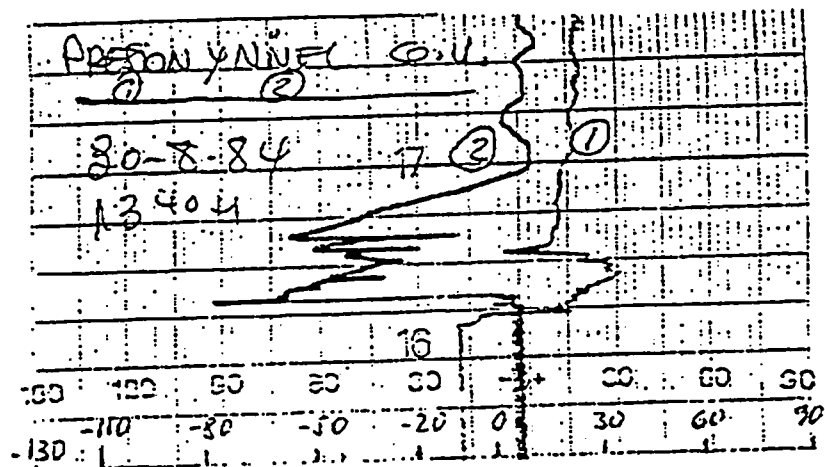


Figure 3.7. Steam Generator Pressure (Kg/cm² rel) & Level (cm rel narrow range).

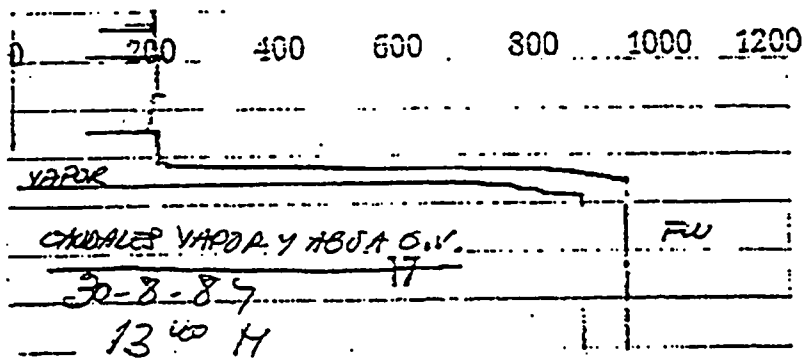


Figure 3.8. Feedwater & Steam Mass Flow Rate (Tonne/h).

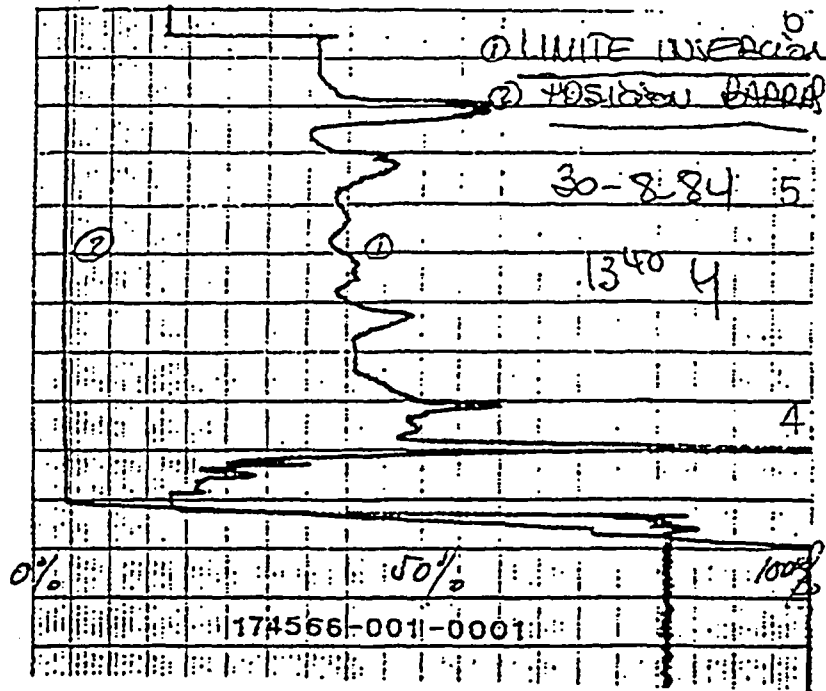


Figure 3.9. Control Rod Position (% of withdrawal) & Insertion Limit (%).

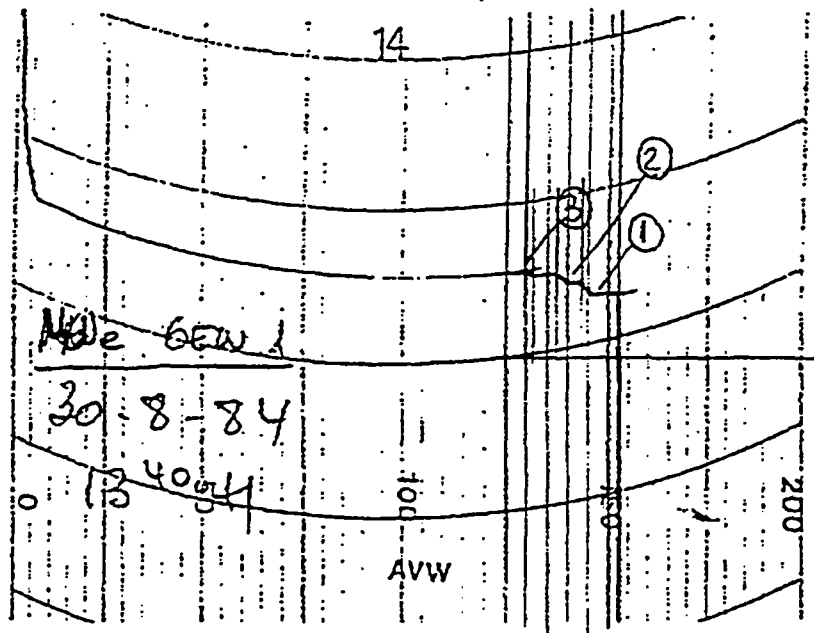


Figure 3.10. Generator Power (MWe).

4. PLANT MODEL AND CODE INPUT DESCRIPTION

For this assessment analysis, the RELAP5/MOD3.2 code /4/ running on a Digital AlphaServer 2000 4/200 computer, under Digital UNIX operating system, has been used.

The RELAP5 model of José Cabrera NPP /6/, /7/ and /8/, depicted in Figure 4.1 is currently being used in Plant Transient and Safety Analysis. The model also includes all the logic necessary to simulate the automatic reactor protection and control system, and many manual actions.

The plant nodalization comprises 167 control volumes or nodes, 29 of them are time dependent volumes, 173 junctions and 109 heat structures. The systems and components included are the following:

- * Reactor Vessel
 - Core and Hot Channel
 - Core and Upper Head Bypasses
 - Upper Head Fans
- * Primary Loop
 - Hot, Cross-over and Cold Legs
 - Chemical and Control Volume System (charging) Pumps and Discharge Orifices
- * Reactor Coolant Pump
 - Four Quadrant Homologous Curves
 - Two-Phase Performance
- * Pressurizer
 - Surge Line
 - Four Heater Banks
 - Spray Line and Valves
 - Heat Losses to Containment
 - Relief and Safety Valves
- * Steam Generator
 - Tubes and Water Chambers
 - Downcomer, Riser, Separator and Dome

- * Steam Lines
 - Safety Valves
 - Steam Dump Valves
 - Isolation Valve
 - Turbine Control and Trip Valves
 - Steam Consumption by EFW Turbine
- * Main Feedwater
 - Piping and Heaters (simplified)
 - Motor Pumps
 - Control, Isolation and Bypass Valves
- * Emergency and Auxiliary Feedwater Pumps
- * Emergency Core Cooling System
 - Safety Injection Pumps
 - Accumulator Tank and Piping

The logic associated with the reactor protection and control system is described by means of 366 control variables and 127 trips. The automatic control systems and signals included are the following:

- * Reactor Scram
- * RCS Average Temperature
 - Control Rod Movement
 - Steam-Dump Valves (only after a turbine trip)
- * Pressurizer Level
 - Charging System
 - Discharge Orifices
 - Heaters
- * Pressurizer Pressure
 - Spray
 - Heaters
 - Relief Valves
- * Steam Generator Level
 - Main Feedwater Control Valve
 - Isolation

- * Turbine Power
 - Turbine Control Valve
 - Turbine trip
- * Safety Injection
- * Emergency and Auxiliary Feedwater

Besides the automatic behaviour, most of the above control systems have provisions, within the model, to allow switching to manual operation mode.

For an easier comparison with plant measurements in assessment cases, the main instrumentation signals in the Control Room have been simulated with their actual units and delays.

5. STEADY STATE CALCULATION

5.1. Steady-State Results

The obtaining of a steady state calculation, as a starting point for the simulation of any transient, is achieved in four steps. The first step is a "new transnt" calculation. The input file contains almost the whole nodalization and fictitious, but faster than real ones, control systems. Once stable and reached the desired conditions, a second step ("restart stdy-st") reduces the restart file size, resets time to zero, and eliminates the fictitious control systems. The third step ("restart transnt") incorporates all the real control systems and reactor kinetics with reactivity feedback coefficients. Finally, a fourth step ("restart transnt") reduces again the restart file size and resets time to zero. After every step, final steady-state is checked.

Parameter	Plant measures/Design values	RELAP5/MOD3.2
Core Power (Mwth)	489.6	439.6
Average Temperature (K)	566	566
Delta T (ΔT , K)	24.2 / 23 (*)	24.3 (**)
PZR Pressure (MPa)	13.83	13.83
PZR Level (%)	62	62.14
RCS Mass Flow Rate (Kg/s)	3780	3769 (**)
RCP speed (rpm)	990 (****)	990 (****)
Charging Flow (lpm)	62	61.92
SG Pressure (MPa)	4.66	4.66
SG Level narrow range (cm rel)	0	0
Steam Mass Flow Rate (Kg/s)	255	254.2 (**)
MFW Mass Flow Rate (Kg/s)	255	254.2 (**)
MFW Temperature (K)	475.3 (****)	475.3 (****)
SG Circulation Ratio (-) (***)	2.04	2.035 (**)

(*) The best-estimate value is 24.2K. The mismatch between the estimated and the registered value is due to thermal streaming phenomena in hot and cross-over legs, and to measurement error as well. The registered value is 23K.

(**) All the figures signed this way are calculated by the code. The other ones are imposed as conditions in the initialization phase.

(***) Circulation ratio = $\dot{m}_{\text{downcomer}} / \dot{m}_{\text{vapor}}$, design value.

(****) Nominal design value

Table 5.1. Steady-state results at 96% nominal power.

Table 5.1 shows a comparison between plant measurements and steady-state calculated results for this transient. Reference values for controlled variables are those corresponding to 96% thermal power. Where measurements were not available, design or historical values were included. Some registered values have been corrected taking into account pen displacements in registers with multiple pens.

5.2. Steady-State Peculiarities

5.2.1. Flow Regime Transitions

While trying to get steady-state conditions, some stability problems arose concerning flow regime transitions. The problems appeared due to uncontrolled jumps from slug to annular-mist flow regimes, just in the two nodes of the riser next to the “U” of the tubes. Several solutions were tried, and the final solution was collapsing the above two nodes in a single node containing entirely the “U” part of the tubes. This solution showed a good behaviour for several steady-state power levels.

The above problem has been traced up to the calculated magnitude of the interphase friction coefficients and interfacial heat transfer coefficients for the different nodes and junctions of the steam generator riser. Tables 5.2 and 5.3 show respectively the SG nodalization parameters and the steady-state results related to this problem. As can be seen within the tables, two abrupt changes exist: one of them between the higher node containing the tubes (bundle flow regime map) and the downstream nodes (pipe flow regime map), another one between the higher node in the straight part of tubes (slug regime) and the next downstream node (annular-mist regime).

These abrupt transitions are responsible of the void fraction profile along the riser. As can be seen in table 5.3, the void fraction is not uniformly increasing from bottom to top. This results in an accumulation of liquid water in the four upper nodes. The total secondary water mass calculated corresponds with the nominal SG water mass given by the vendor, which is 10% greater than that obtained with RELAP5/MOD2.5 (see table 8.1).

5.2.2. Pressure Losses

Due to some changes in the way the pressure losses are calculated by RELAP5/MOD3.2 with respect to those calculated RELAP5/MOD2.5, readjusting the overall pressure losses of both primary and secondary circuits was necessary. This was accomplished by slightly changing the form loss coefficients at junctions.

5.2.3. Steam Generator Pressure

The secondary sides of heat structures representing the steam generator tubes were modeled with bundle geometry. The hydraulic diameter for heat transfer was calculated, as usual, considering only one quadrangular cell of four tubes. The pitch/diameter ratio was selected to be the actual one. Finally, the "fouling factor" was tuned to match the nominal steam generator pressure.

Secondary side pressure is a function of the operation power, SG tube fouling and thermal streaming phenomena in the primary side. Thermal streaming is not possible to be simulated with a 1-D code, because of its 3-D intrinsic nature. This thermal streaming is due to the turbulent mixing of the core outlet temperature distribution in the hot leg and due to the different cooling lengths inside the steam generator tubes in the cross-over leg. This results in a difference between instrumented average temperature and "actual" average temperature.

In order to get the correct value, the fine tuning of the secondary side heat transfer coefficient was reached by a little adjustment of the so called "fouling factor" to take into account the aforementioned phenomena. That factor is actually a multiplier, so it can increase or decrease the value of the calculated heat transfer coefficient.

Node						Junction				Heat Structure (cylindrical)					
Number	Λ (m ²)	L (m)	V (m ³)	ϕ_{H} (m)	Option	Number	Λ (m ²)	ϕ_{H} (m)	k	Number	ϕ_{H} (m)	Factor (m tube)	Option		
400-08	2.87	0.724	2.083	1.0095	pipe										
400-07	4.91	0.636	3.128	2.51	pipe	400-07	2.87	1.0095	2.64						
400-06	4.06	1.273	5.169	0.0375	bundle	400-06	4.06	0.0375	2.64	120-09		0.0375	1588	bundle	
400-05	3.49	0.8288	2.893	0.0375	bundle	400-05	3.49	0.0375	2.64	120-08		120-10	0.0375	2158	bundle
400-04	3.49	0.8288	2.893	0.0375	bundle	400-04	3.49	0.0375	2.64	120-07		120-11	0.0375	2158	bundle
400-03	3.49	0.8288	2.893	0.0375	bundle	400-03	3.49	0.0375	2.64	120-06		120-12	0.0375	2158	bundle
400-02	3.49	0.8288	2.893	0.0375	bundle	400-02	3.49	0.0375	2.64	120-05		120-13	0.0375	2158	bundle
400-01	3.49	0.8288	2.893	0.0375	bundle	400-01	3.49	0.0375	2.64	120-04		120-14	0.0375	2158	bundle
401-02	3.49	0.699	2.4401	0.0375	bundle	369	3.49	0.0375	2.64	120-03		120-15	0.0375	2158	bundle
401-01	3.49	0.608	2.1225	0.0375	bundle	401-01	3.49	0.0375	2.64	120-02		120-16	0.0375	1820	bundle
										120-01		120-17	0.0375	1583	bundle

Table 5.2. Steam Generator Riser: Main Nodalization Parameters

Node							Junction					Heat Structure (cylindrical)						
Number	voldg	quale	vapgen (Kg/s·m ²)	hlf (**) (w/m ² ·K)	hfg (***) (w/m ² ·K)	Regime	Number	flj (N/s ² ·m ²)	velf (m/s)	velg (m/s)	Regime	Number		Q̇ (w/m ²)		Regime (*)		
400-08	0.64	0.51	-0.002	7.1E6	4.2E5	ANM												
400-07	0.53	0.51	-0.001	4.2E5	1.3E4	SLG	400-07	2.7E1	0.24	7.3	ANM							
400-06	0.75	0.51	8.2	4.3E7	1.5E6	ANM	400-06	1.4E2	0.32	3.7	ANM	120-09		2.4E5		3		
400-05	0.74	0.43	13.3	3.3E7	6.4E5	SLG	400-05	1.4E2	0.42	3.6	SLG	120-08		120-10	2.5E5	2.3E5	3	3
400-04	0.86	0.35	13.3	2.9E7	6.5E5	SLG	400-04	1.5E3	0.93	2.6	SLG	120-07		120-11	2.6E5	2.2E5	3	3
400-03	0.84	0.28	13.4	2.5E7	4.3E5	SLG	400-03	1.2E4	0.91	2.1	SLG	120-06		120-12	2.7E5	2.E5	4	4
400-02	0.78	0.21	13.6	2.8E7	3.7E5	SLG	400-02	1.7E4	0.71	1.6	SLG	120-05		120-13	2.9E5	1.9E5	4	4
400-01	0.68	0.13	13.2	1.9E7	2.7E5	SLG	400-01	2.8E4	0.52	1.2	SLG	120-04		120-14	3.1E5	1.8E5	3	3
401-02	0.49	0.005	10.5	9.7E5	1.7E5	SLG	369	5.0E4	0.35	0.74	SLG	120-03		120-15	3.3E5	1.7E5	3	3
401-01	0.11	-0.001	2.01	3.9E5	2.0E5	BBY	401-01	3.6E4	0.21	0.48	SLG	120-02		120-16	3.5E5	1.6E5	3	3
												120-01		120-17	3.8E5	1.6E5	3	3

(*) 3: subcooled nucleate boiling, 4: saturated nucleate boiling

(**) hlf: bulk interfacial heat transfer for liquid phase.

(***) hfg: bulk interfacial heat transfer for vapor phase.

Table 5.3. Steam Generator Riser: Flow Regime Related Results.

6. TRANSIENT ANALYSIS

This section describes, with some detail, the transient simulation results. It contains an explanation of the evolution and behaviour of main variables, like pressures, temperatures and levels.

The following three subsections, first, summarize the sequence of events, second, analyze the plant response to control system actuation and manual actions, trying at the same time to extract conclusions about RELAP5/MOD3.2 performance and about plant model adequacy, and third collects some data about run statistics.

6.1. Sequence of Events

Table 6.1 shows the timing of the transient and some comments with respect to the plant response after the initiating event and after every manual action.

The plant registers included in the "Reactor Trip Report" (Figures 3.1 to 3.10), as was said above, are somewhat imprecise about the timing of the transient and about the value of some variables. So, the timing of the transient included in Table 6.1 is a compromise among different registers. This compromise was obtained after a careful analysis of registers and after many calculations, accompanied by cross-comparisons between calculated variables and registered ones.

Time (s)	Event	Remarks
0	PZR Spray valve opening	Starting of PZR pressure decrease. Slight moderator density decrease and therefore slight nuclear power decrease. This produces a slight decrease of average temperature and SG pressure. Slight opening of turbine control valve.
30	Backup Heaters ON	PZR pressure < 13.58 MPa setpoint reached
290	Starting of Turbine Load reduction	4%/minute. Turbine control valve throttling. SG pressure increase and MFW flow decrease to maintain SG level. Average temperature increase along with programmed temperature decrease start control rod insertion. PZR pressure continues decreasing.
520	Reactor SCRAM caused by low PZR pressure	PZR pressure < 12.41 MPa. Associated turbine trip. Steam-dump in auto mode leads average temperature down to the no-load reference (548.15 K). SI signal by PZR pressure < 11.72 MPa.
540	Manual actions immediately following reactor trip	MFW isolation (valve closing time 139 s).
560		PZR reference level to manual (35%).
570		Steam-dump switched to pressure (manual) mode.
580		One MFW pump is tripped.
600		Second charging pump at max flow.
600 ÷ 1493	Manual control trying to stop PZR pressure decrease	MFW isolation bypass valve to recover SG level. Steam-dump to rise RCS average temperature. Charging flow to recover PZR level. PZR pressure continues decreasing.
1493	RCP trip	Just before reaching SI pumps shut-off pressure (9.5 MPa). Stops spray flow and therefore PZR pressure decrease. Natural circulation.
2500	End of simulation	Main plant variables recovered and controlled. PZR pressure being recovered by heaters.

Table 6.1. Sequence of events for the simulated transient

6.2. Plant Response to Control System Actuation

Up to the reactor trip, the control systems worked in automatic mode. After the trip, they worked in manual mode under operator control. Due to some uncertainties in the value of reference points with which the control systems were operated, and the lack of some references about the timing of manual actions, those parameters were deduced only after many calculations and after a careful analysis of plant registers. The result of this process has been a coherent and acceptable evolution of calculated variables in comparison with registered ones.

The manual operation of some control systems was simulated to match registered values of controlled variables (i.e. feedwater flow to match steam generator level), which is summarized in the following paragraphs. When differences between expected, or registered, and simulated behaviours are important, they include a possible explanation of those differences, whichever its cause will be: plant register uncertainties, plant model nodalization, or code performance.

6.2.1. Turbine Control Valve

During the first 290 s of the transient, the control system of this valve was operating automatically with a constant reference power of 96%. Therefore the valve slightly opened (Figure 6.20) to maintain the steam flow (Figure 6.7), which tended to decrease in response to the nuclear power decrease (Figure 6.12), caused by the reactivity change (Figure 6.21) derived from the RCS pressure decrease (Figure 6.1).

From 290 to 520 s the operator began a turbine load reduction at an average rate of 4%/minute (from 96 to 81% power). So, the throttling of the turbine control valve (Figure 6.20) produced a pressure increase in the secondary circuit (Figure 6.5). The only indication about the load reduction rate, and its corresponding steam flow rate reduction, is the output electrical power register (Figure 3.10), because the steam flow record (Figure 3.8) is very imprecise due to pen displacements. The agreement between calculated and registered SG pressure before the reactor trip (Figure 6.5), certifies the adequacy of the simulated flow reduction (from 96% to 80% flow rate).

The reactor trip, at 520 s, induced the turbine trip signal, which closed the turbine stop valve (closing time of 0.15 s). This steam flow cutting produced a calculated initial SG peak pressure of about 5.79 MPa, which compares well with the plant record (Figure 6.5).

6.2.2. Pressurizer Pressure Control

The pressurizer pressure control system was operating automatically during the whole transient. Its behaviour was as expected. From the beginning of the depressurization transient, PZR control heaters increased their power continuously (Figure 6.9) following the compensated pressure error signal. At a calculated time of 30 s, the PZR pressure crossed the 13.58 Mpa setpoint, switching on the backup heaters.

After the activation of the SI signal (PZR pressure < 11.72 MPa), the backup heater group "B2" is automatically disconnected (at 540 s). If the SI signal is not manually reset, this situation would remain. This resetting was assumed to happen at 1600 s, which is necessary to match the registered recovering slope of the PZR pressure (Figure 6.1). After the RCP trip, the calculated pressure slope must follow the registered one, because the spray flow has ceased (Figure 6.15) and the average temperature (Figure 6.3) and PZR level (Figure 6.2) are nearly constant and stable, which are correctly reproduced.

6.2.3. Pressurizer Spray Valve

The spray valve behaviour during the transient was simulated taking into account the following considerations: a) the initiating event was a failure in the driving mechanism of this valve, the nature of this failure introduces a certain degree of uncertainty on the actual valve position during the transient, because the only available indication is the demanded position, which was always zero, b) the mass flow rate at its maximum opening is not well known, and c) the timing of the main events is rather imprecise due to plant registers uncertainties.

Therefore, it was decided to carry out the transient simulation without any restriction on the spray valve position or mass flow rate. This valve position was adjusted to match the registered PZR pressure evolution (Figure 6.1). This strategy was

accompanied, to get some insights, with an acceptable simulation of the pressurizer level (Figure 6.2). The resultant spray flow is shown in Figure 6.15.

After the reactor trip, the PZR pressure decreases, and the subsequent evolution was matched forcing the spray valve flow, increasing immediately after trip and reducing it after that. This fact could be attributed mainly (see Sections 7.3 and 7.4), without discarding the influence of other effects (i.e. differences between the recorded and the actual average temperature and timing uncertainties), to RELAP5 condensation modelling of the spray.

When the pressurizer level reach the node where the spray nozzle is located, this is at a level of 71% (Figure 6.2), the condensation due to the spray (Figure 6.28) does not cease or become unstable, as in previous code versions (see Section 8), which is a clear improvement of MOD3.2.

Section 7 below includes some sensitivity calculations on the PZR response, with the intention of evaluating the influence of the various factors quoted at the beginning of this subsection. Section 8 also includes a comparison with MOD2.5 results.

On the other side, it has to be taken into account that RELAP5 has not a specific model for sprays. The spray real behaviour is a function of flow rate, water temperature, initial droplet diameter and the nozzle elevation above the liquid surface. The droplets enter into the pressurizer at cold leg temperature, and the vapor in the pressurizer condenses on the droplets in their way to the level surface. The droplets temperature rises up to the saturation temperature, their condensation capability disappearing from that time on. In any case, they also disappear when they reach the level surface. All these effects are essentially non-local. That means that there are spray effects between the spray nozzle and the level surface, wich could affect several nodes. RELAP5/MOD3.2 does not have a representation of droplets fields, being the spray inlet node properties an average of inlet spray flow and vapor in PZR. The main effect is that this approach is not sensitive to PZR level position, what makes necessary and justifies the strategy above described.

6.2.4. Pressurizer Level Control

The pressurizer level control system is composed of two charging pumps. One of them operates automatically, being its velocity a function of the level error signal. The other pump, which is normally stopped, can be manually started and controlled. The PZR level follows a programmed level, which is a function of the RCS average temperature. This reference level can also be switched to manual setting.

This control system was operating in automatic mode from the beginning of the transient up to the reactor trip. During this time, the make-up flow decreased following the level error signal, which increased continuously. The predicted values compare acceptably with the registered ones (Figures 6.2 and 6.8).

After the reactor trip (occurred at 520 s), the system was operated in manual mode. The exact timing of manual actions and the value of manual setpoints is not well referenced, so they were deduced during the calculation process. The strategy was to match the registered PZR level evolution (Figure 6.2) while maintaining an acceptable prediction of the average temperature (Figure 6.3). This was accomplished by the following assumptions: 1) at time 560 s, the programmed level setpoint was fixed at a value of 35%, 2) at time 600 s, the manual charging pump, which was started certain time before the reactor trip, begins to introduce water at its maximum rate, 3) at time 900 s the automatic charging pump is stopped, 4) from time 960 s on, with the PZR level at 64% and increasing, the velocity of the manual charging pump is reduced and controlled to give a flow rate around the let-down one.

Those above assumptions and strategy correspond to a charging mass flow rate which compares acceptably with the measured one (Figure 6.8). For a better interpretation and evaluation of the data included in this figure, the following remarks could be helpful: a) the “net inflow”, which equals the let-down flow in steady-state conditions, includes the charging line flow and the fraction of the RCP seal flow leakage to the RCS, b) the charging-flow represents the plant measurement, which does not include the seal flow, c) the charging flow-meter (Figure 3.6) has an upper scale limit below the actual maximum flow, this limit is overcome when both charging pumps operate together, d) the evolution

of seal flow and discharge flow during transient conditions is not included in the model, introducing a certain degree of uncertainty on the results.

Operator actions may be interpreted as follows. After the reactor trip, the operator began to introduce water in the RCS at the maximum possible rate, first to rapidly recover the PZR level and second to stop the pressure decrease. But the pressure (Figure 6.1), after a certain time of stabilization, went down again. This last fact is due to the evaporation/condensation phenomena in the pressurizer (Figures 6.29, 6.30 and 6.31), as is explained below.

After the trip, the depressurization due to the rapid level decrease, because of the primary coolant contraction, is attenuated by a net evaporation rate peak. Then the pressure is stabilized by the water incoming from the surge line and the evaporation rate at the wall, which counteract the spray condensation. Then, with the level recovered at a time next to 1000.s, the make-up flow is reduced to letdown flow, but the surge line inflow remains because of an increasing average temperature. In spite of this inflow, the pressure begins to decrease again because the wall evaporation rate has diminished to that due only to heaters, and both effects are unable to counteract the spray condensation rate.

The pressurizer level evolution after the make-up flow reduction follows the average temperature evolution. The little make-up flow variations after that time are attributed to variations in the RCP seal and return flows, which indeed are due to variations in the CVCS Tank conditions.

The calculated minimum level after the reactor trip is somewhat higher, 5%, than that in plant data. This discrepancy could be attributed to the RCS average temperature uncertainty. As was said, after the reactor trip the actual average temperature could have been less than the registered one.

6.2.5. Control Rod Motion

The average temperature control system is responsible of the control rod motion, to maintain that temperature within the deadband margins ($\pm 1.4\text{K}$) of the reference

temperature, which is a function of the turbine load.

After the beginning of the turbine load reduction, the control rods began to be inserted when the temperature error signal surpassed the deadband margin (Figures 6.3 and 6.19). The insertion velocity was the minimum, because it is determined by a combined temperature error, composed of a temperature error term plus a pressure error term. The sign of the last term was always opposite to the sign of the first, and its value high enough to maintain the velocity at the minimum value (see Reference 1).

The reactor power response to the control rod insertion (negative reactivity) is not a recorded data, so the goodness of the calculated one can only be indirectly evaluated through the average temperature evolution (Figure 6.3), which compares well with that registered.

The input reactivity feedback coefficients were calculated from reactor core design data of the cycle corresponding to the present transient.

6.2.6. Steam-dump Control

The steam-dump control system of José Cabrera NPP only operates after a turbine trip. It has two modes of operation: temperature or pressure control. The temperature mode control is designed to get the no-load average temperature in the primary system (548.15K). The pressure control mode is designed to follow a manually selected steam generator pressure setpoint, and it can only be activated below 15% turbine power.

For the present transient, the system was switched to pressure mode at a certain time after the turbine trip. This time is not well referenced in the "trip report", so it was deduced during the calculation process. This action was taken to rise the primary system average temperature, trying to stop the pressurizer pressure decrease.

The strategy of the calculation was to match the RCS average temperature. This was achieved (Figure 6.3) first by determining the time when the system was switched to pressure mode, and then by finding the SG setpoint evolution during the transient.

The above strategy was adopted after a first round of calculations, which showed a lack of coherence between both calculated and recorded SG pressure and average temperature. If the SG pressure was matched, the average temperature resulted too low (2-3K), and when matching temperature resulted in a SG pressure too high (2-3 bar). Those differences were only significant in the time interval from the reactor trip to turbine trip, while outside this time matching was acceptable.

On the other side, hot and cross-over leg streaming effects could have a major influence in this behaviour. Average temperature is calculated by a combination of three thermocouples measurements in the hot leg and three in the cross-over leg. The auctioneer logic takes the largest one (which is a conservative assumption to anticipate the actuation of the Control and Protection System). Because of thermal streaming, there could be a bias between measured and real average temperatures, this bias being a function of the nuclear thermal power.

The average temperature measurement drives some important control systems, like steam-dump and PZR reference level. So, it was considered necessary to match the registered average temperature, at least up to the time those systems are switched to manual mode after the reactor trip. Also, at the beginning of the calculation process, it was unknown if the lack of coherence was due to the measurements, registers, nodalization or code models. So, those reasons justified the adopted strategy.

Nevertheless, with that strategy, the steam generator pressure trends and slope changes are well predicted (Figure 6.5) within the above explained time span.

Section 7 contains a sensitivity calculation with the recorded SG pressure as the matching objective, it also includes some interesting comments about the uncertainty associated with the average temperature measurement.

The temperature prediction while the system was in automatic mode, this is between the reactor trip (520 s) up to 570 s is quite good (Figure 6.3). The same can be said about the steam generator pressure (Figure 6.5) including the peak that happen just after the reactor trip.

The steam generator response to sudden changes in the steam-dump flow, which are originated by setpoint changes, is predicted correctly. Those changes occur between 1450 and 1600 s (Figure 6.11) a. They promote rapid increases in the SG level which are well predicted in comparison with plant data (Figure 6.6).

6.2.7. Steam Generator Level Control

This system is designed to maintain the steam generator level at a constant reference level of 0 cm rel., which is equivalent to 8.931 m over the tube plate. This is accomplished by actuating the main feedwater control valve position. This position is a function of level deviation and steam-feedwater flow mismatch.

When the plant is operating at power, this system operates automatically, but after a turbine trip the system is usually operated under manual control to avoid excessive cooling of the primary system. The following manual actions are taken immediately after a trip: 1) one MFW pump, is stopped, 2) the MFW isolation valve is closed, 3) the MFW control valve is fixed in its minimum position, and 4) the SG level is manually controlled by opening the isolation bypass valve.

For the present transient, the system was operating automatically before the trip, and all the above actions were taken after it. The timing of those actions was not referenced with precise values in the "Trip Report". So, both timing and bypass valve opening were deduced during the calculation, trying to match the recorded SG level after the reactor trip.

After the trip the calculated steam generator level follows acceptably the measured one (Figure 6.6). Otherwise, the calculated level evolution during the turbine load reduction phase of the transient could be unrealistic. As can be seen in Figure 6.6, the calculated level has a sharp peak which does not appear in the plant record. After in depth analysis, it was concluded that the abrupt transitions among flow regimes may be responsible of this behaviour (Figures 6.25 and 6.26). Section 7 contains a sensitivity analysis in which the transition from slug to annular-mist flow regime has been smoothed, showing a better behaviour of the level.

Therefore, with that level evolution before the reactor trip, the calculated main feedwater flow also shows an abnormal behaviour (Figure 6.7). The registered steam flow after the reactor trip is also shown in Figure 6.7.

It is important at this point to remember that, the MOD3.2 steady-state gives a SG secondary water mass near to 10% more (which is the vendor figure) than MOD2.5.

6.2.8. RCP Manual Trip

Once the PZR spray valve failure was clearly identified, the RCP was tripped (~1500 s) to stop the spray flow. After this trip, the primary system flow (Figure 6.16) decreased following the coast-down curve. After approximately three hundred seconds a stable natural circulation regime was established, being its flow high enough to maintain an adequate subcooling margin (Figure 6.4).

As can be seen in Figure 6.17, the Delta T plant data is well reproduced by the code. The differences, even in the peak after the RCP trip, could be attributed to both hot and cold leg thermal streaming. The largest difference between plant data and calculated data is reached when the main coolant pump is restarted. This could be explained for the transition between forced convection and free convection patterns, which could affect the cross-over leg temperature measurements.

After the RCP trip, the pressurizer pressure began to be recovered by PZR heaters under automatic control (Figures 6.1 and 6.9). The initial hot leg temperature increase (Figure 6.4) was manually mitigated by increasing the steam-dump flow (Figure 6.11). Once obtained the desired subcooling, the average temperature was maintained around a constant value (Figure 6.3).

6.3. Run Statistics

The base case of the transient was ran on a Digital AlphaServer 2000 4/200 computer under DIGITAL UNIX operating system.

The numerical scheme used in RELAP5/MOD3.2 was the one corresponding to the number 7, this is semi-implicit and coupled thermalhydraulics.

The maximum timestep allowed during the calculation was 0.05 seconds, which was always taken, except just after reactor trip. The consumed CPU time was 4258 seconds, which gives a CPU to real time ratio of 1.7/1.

Figure 6.1.- Pressurizer Pressure

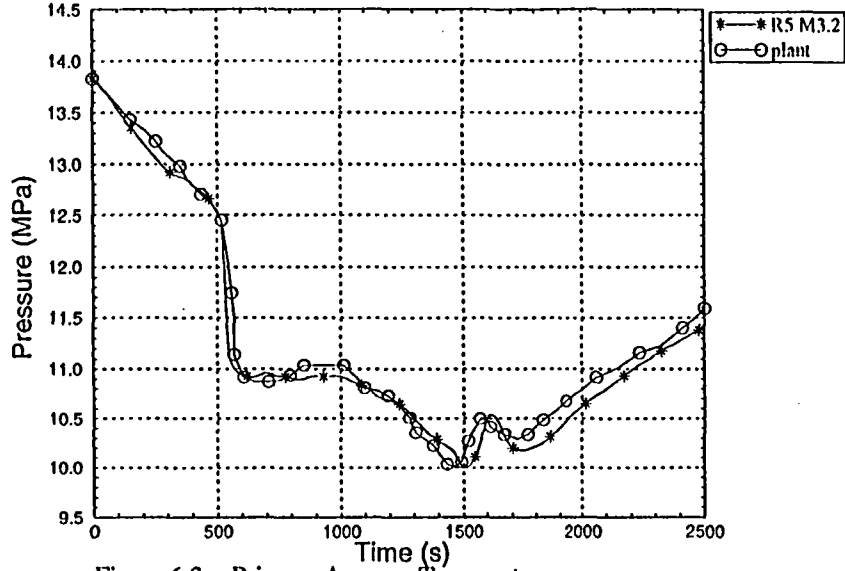


Figure 6.2.- Pressurizer Level

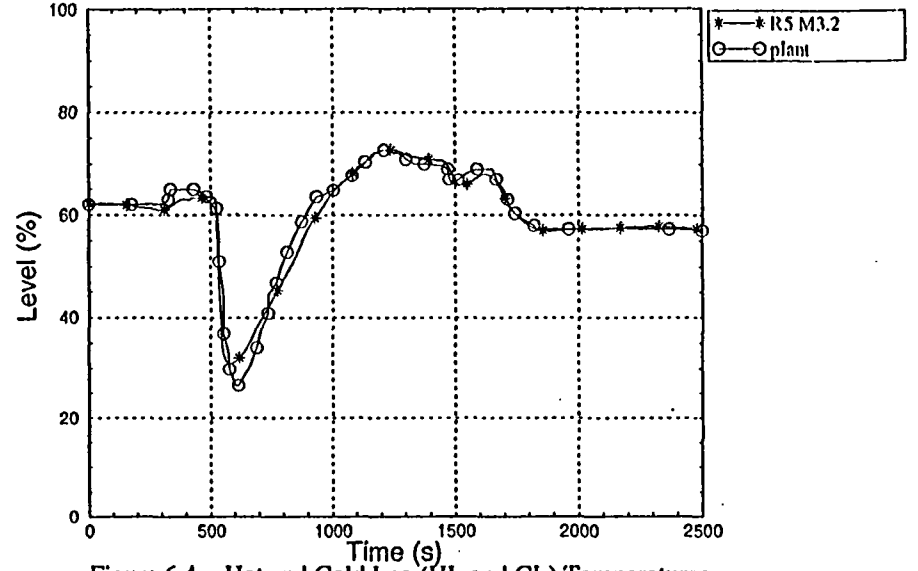


Figure 6.3.- Primary Average Temperature

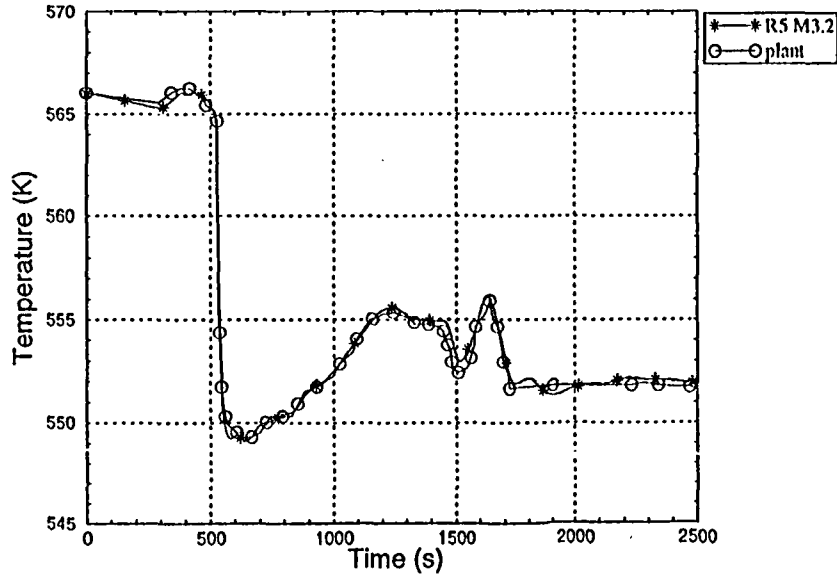


Figure 6.4.- Hot and Cold Leg (HL and CL) Temperatures

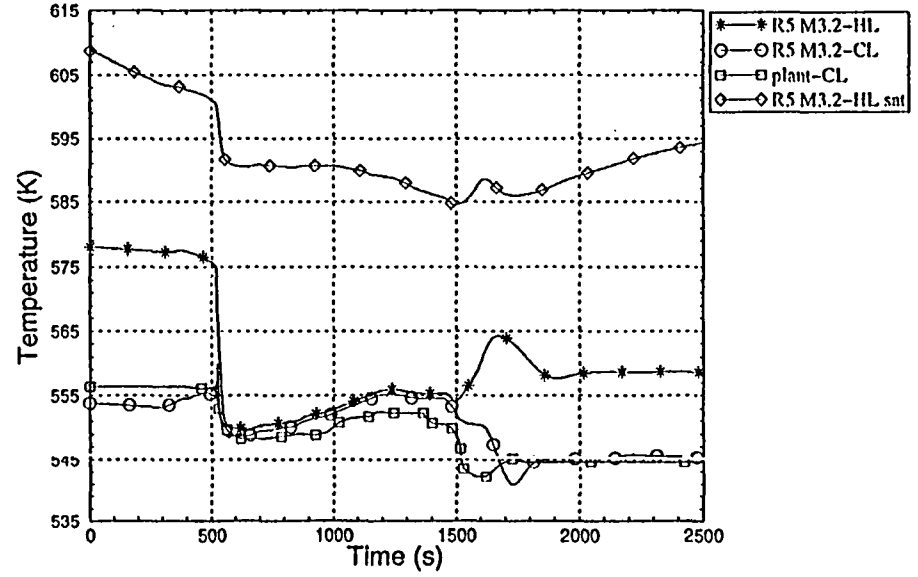


Figure 6.5.— Steam Generator Pressure

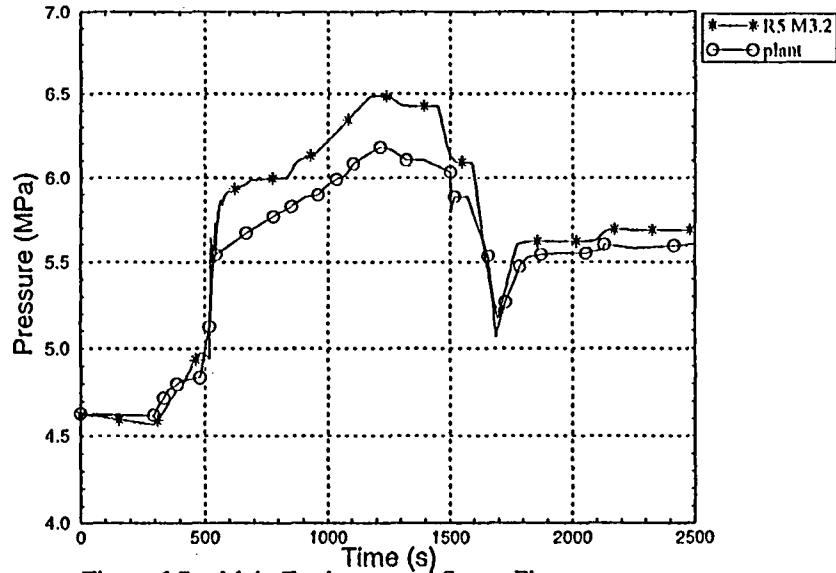


Figure 6.6.— Steam Generator Level (Narrow Range)

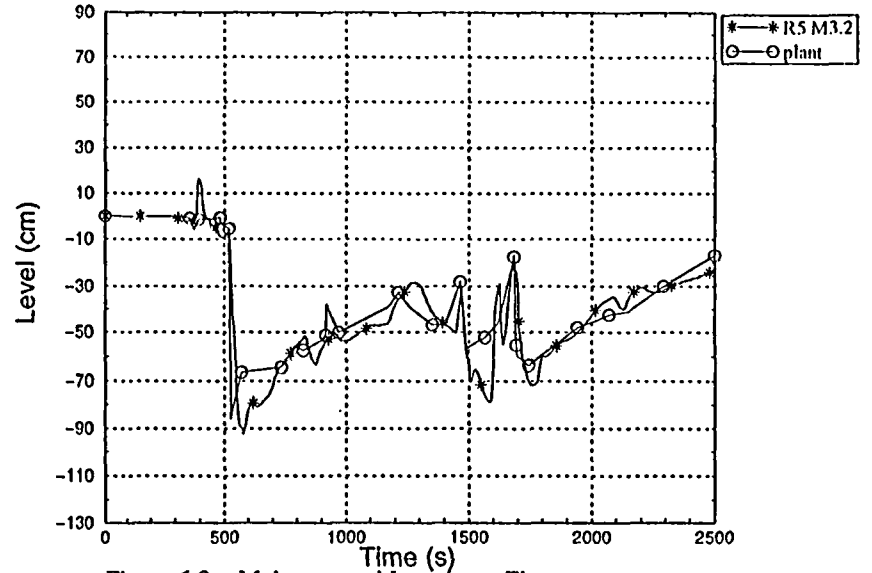


Figure 6.7.— Main Feedwater and Steam Flows

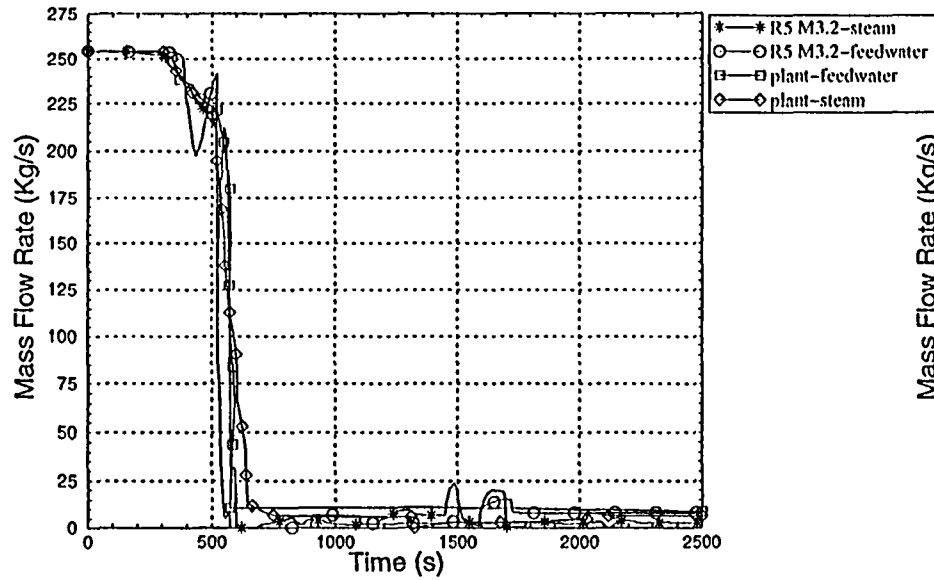


Figure 6.8.— Make-up and Let-down Flows

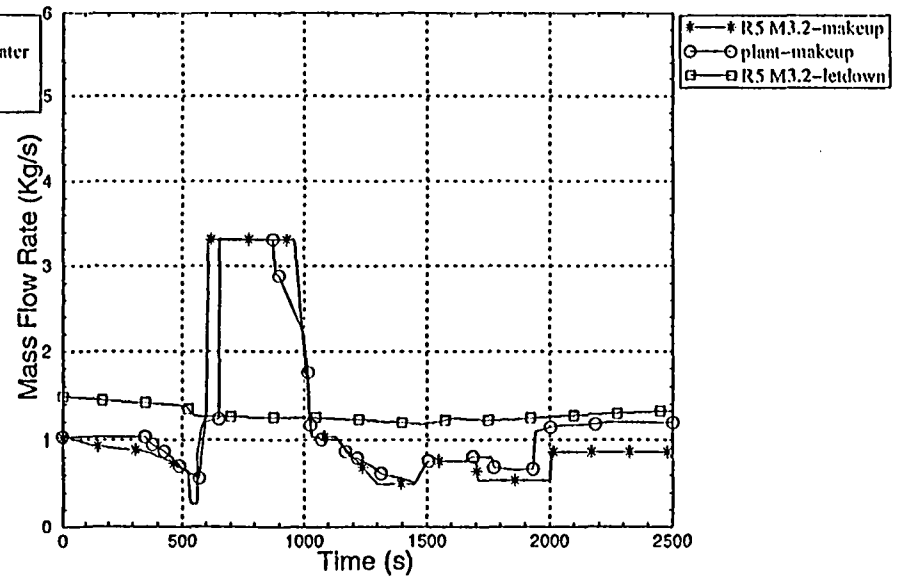


Figure 6.9.— Pressurizer Heaters Power

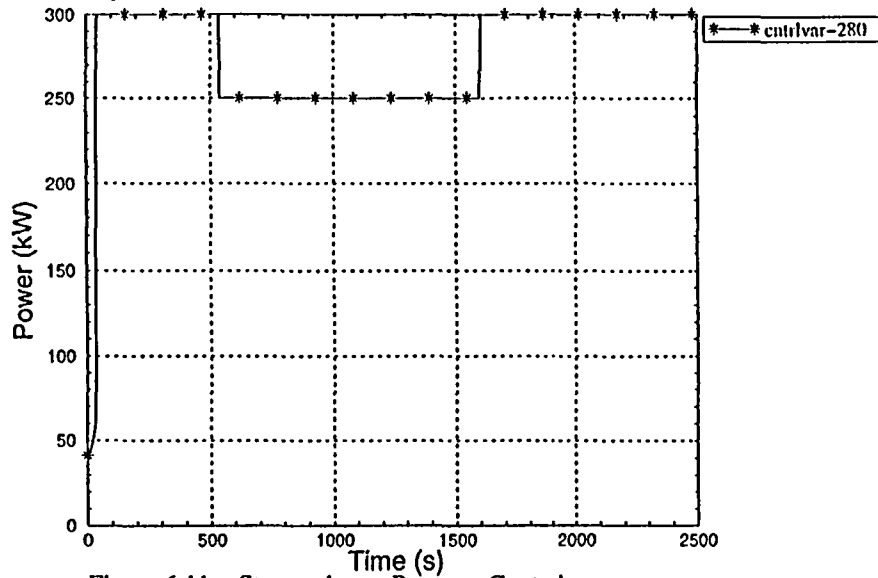


Figure 6.10.— Steam-dump, Tavg Control

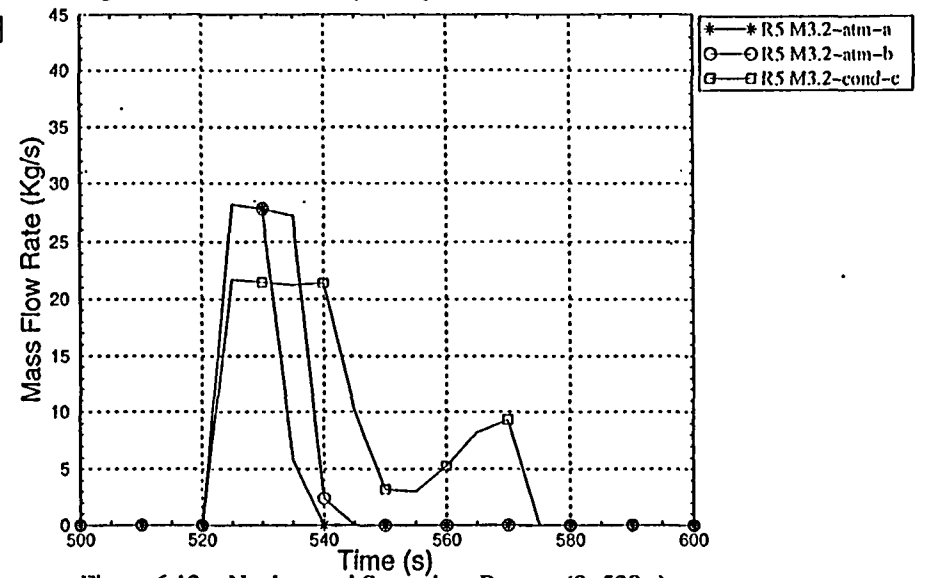


Figure 6.11.— Steam-dump, Pressure Control

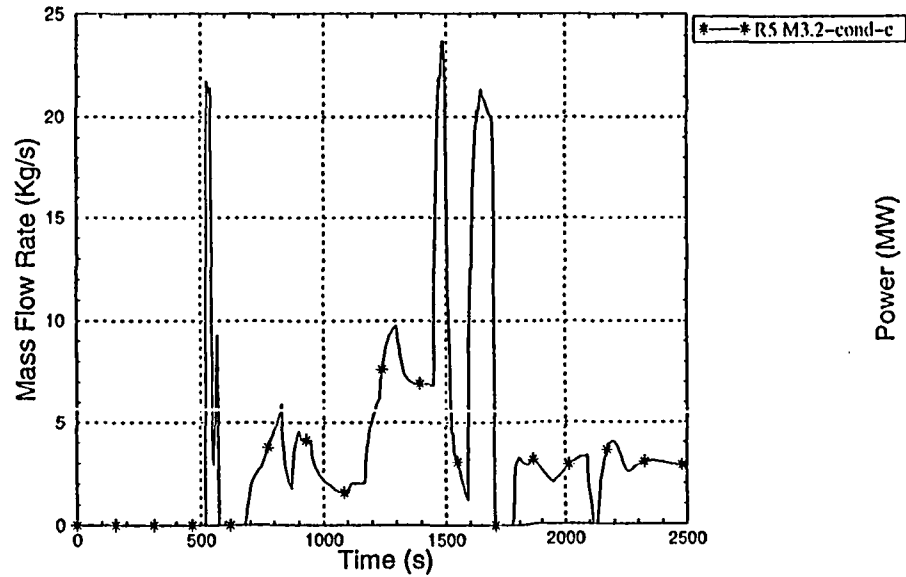


Figure 6.12.— Nuclear and Secondary Powers (0–520 s)

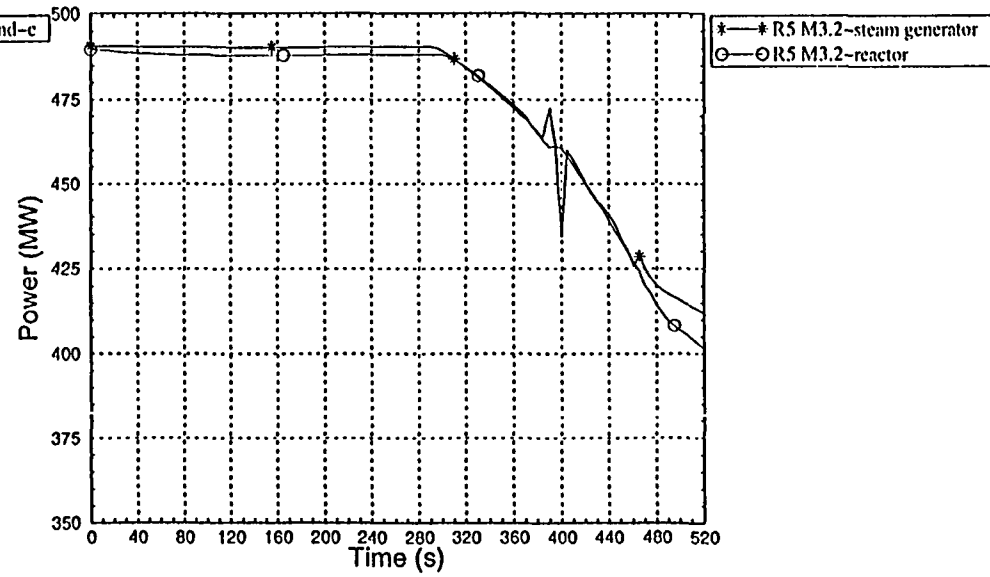


Figure 6.13.- Nuclear and Secondary Powers

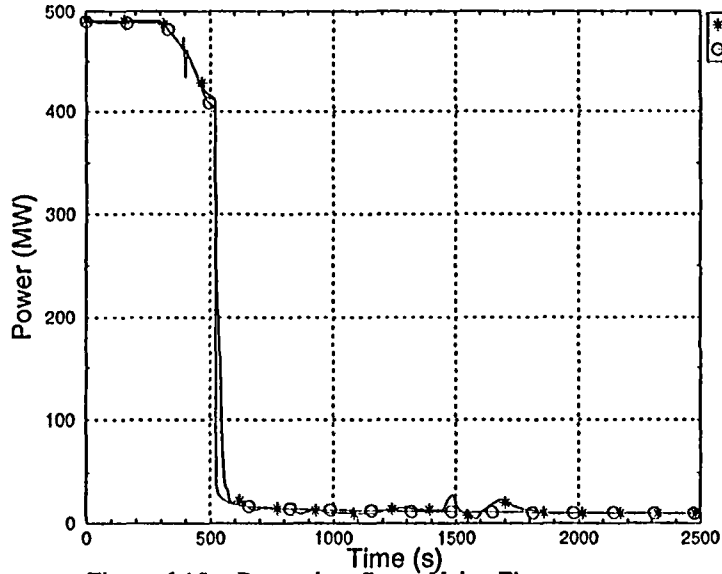


Figure 6.14.- Primary-Secondary Temperature Difference (K)

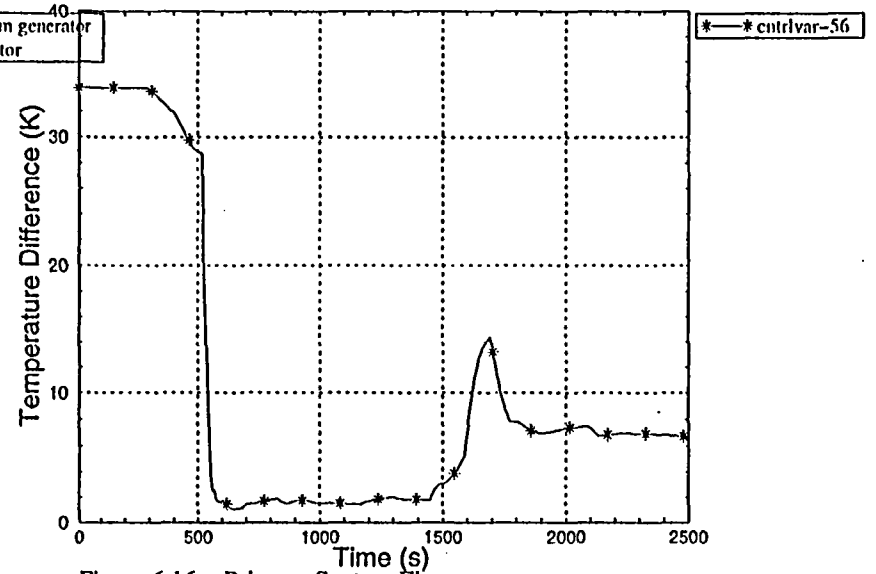


Figure 6.15.- Pressurizer Spray Valve Flow (Kg/s)

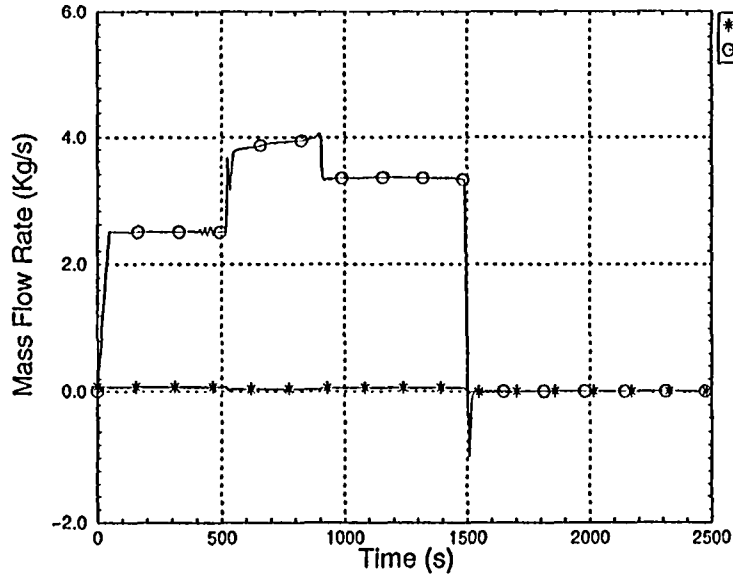


Figure 6.16.- Primary System Flow (Kg/s)

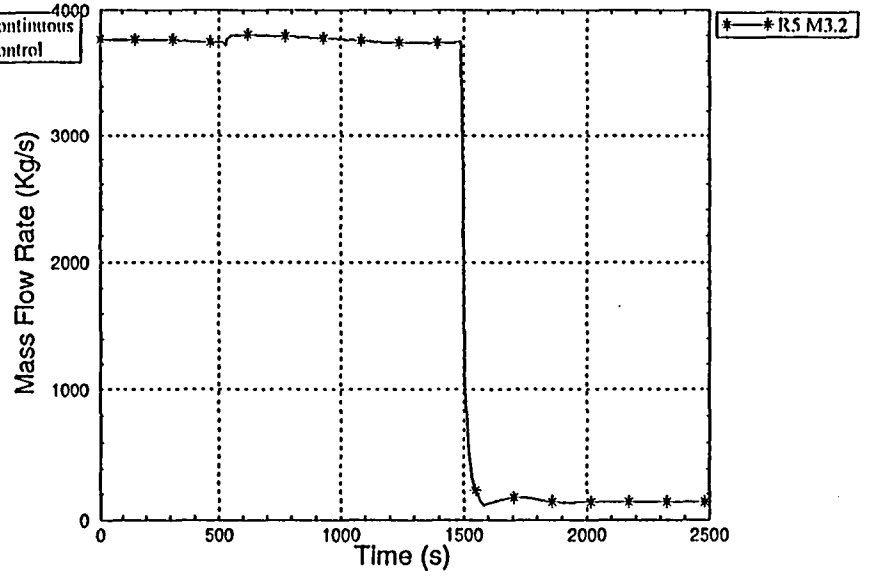


Figure 6.17.- Primary System Delta T

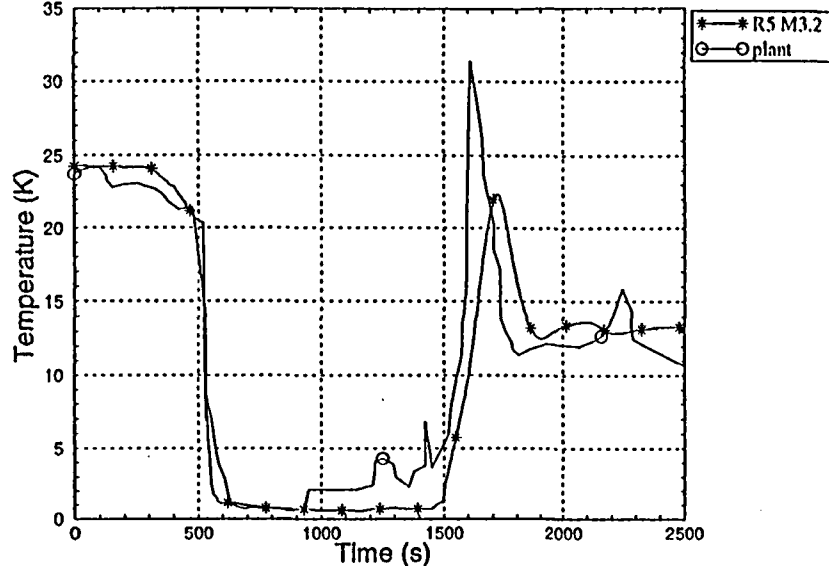


Figure 6.18.- Feedwater Temperature

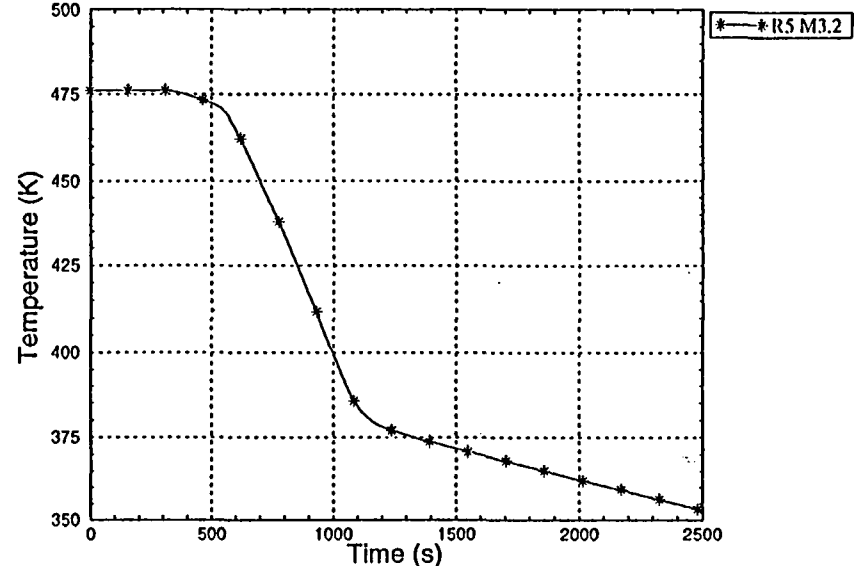


Figure 6.19.- Control Rod Position

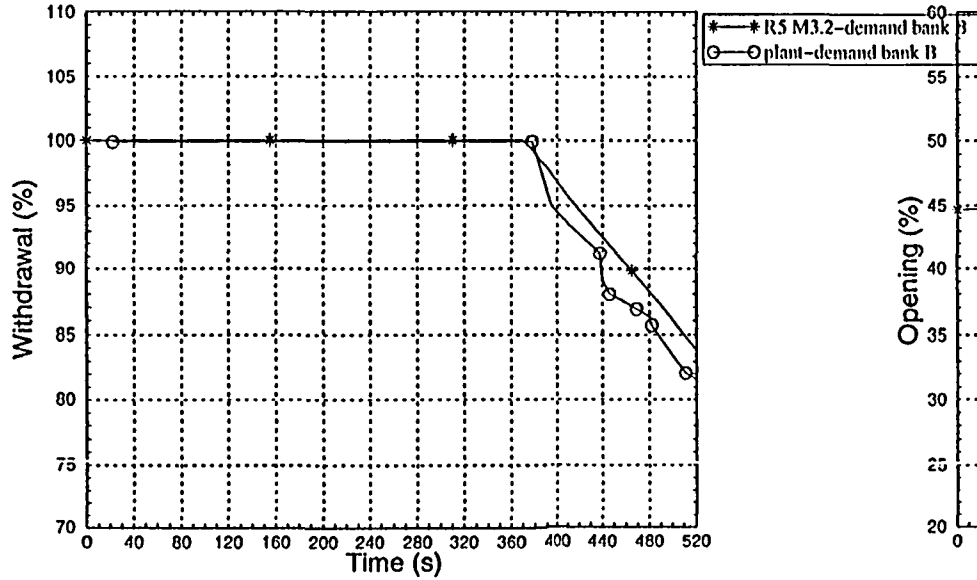


Figure 6.20.- Turbine Control Valve Opening

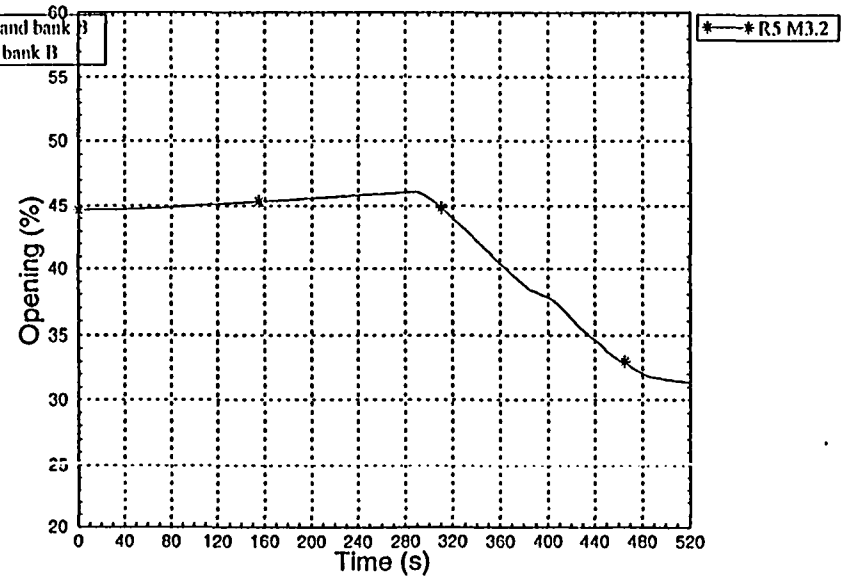


Figure 6.21.- Core Reactivity Contributions

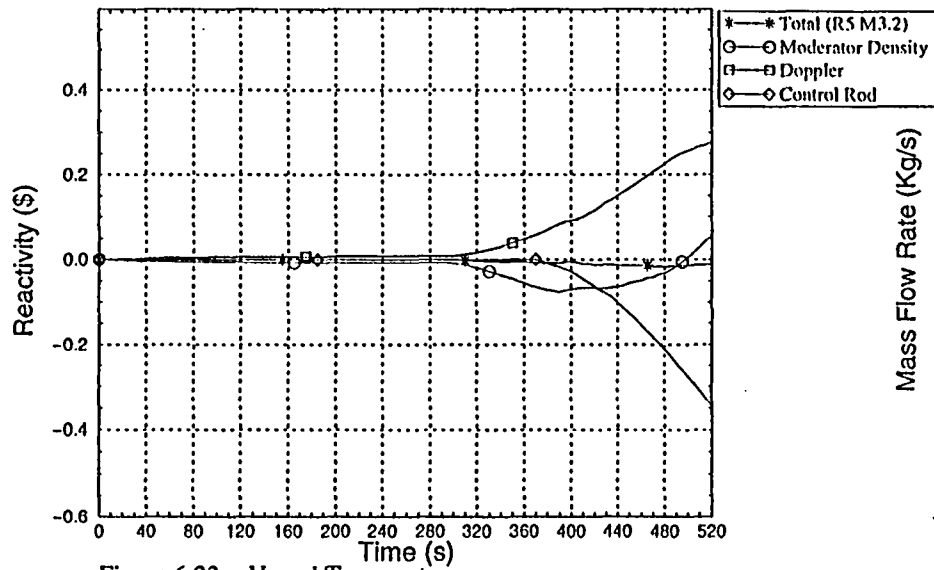


Figure 6.22.- Vessel Head Flows

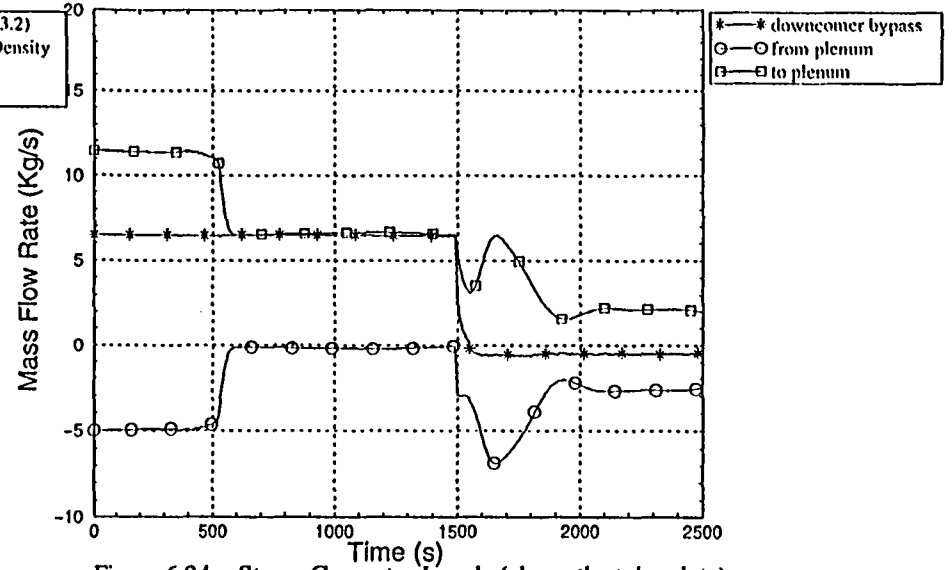


Figure 6.23.- Vessel Temperatures

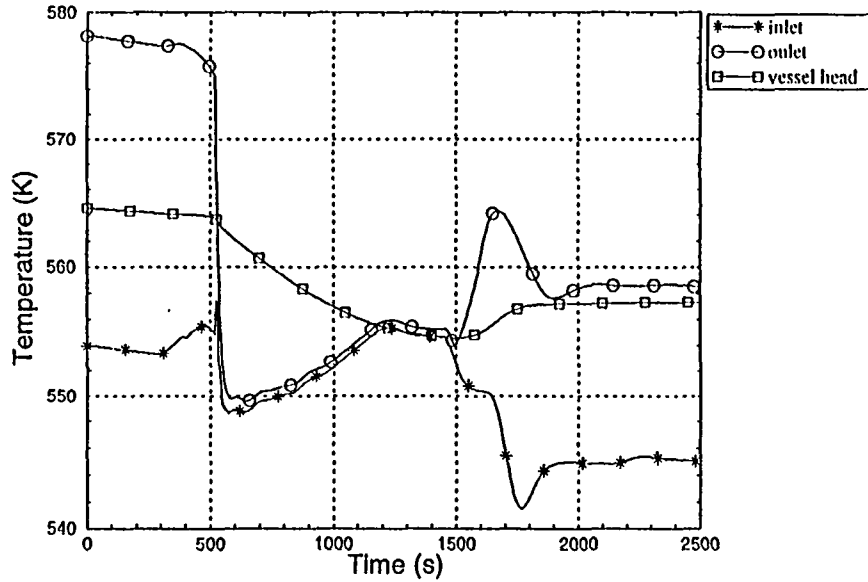


Figure 6.24.- Steam Generator Levels (above the tube plate)

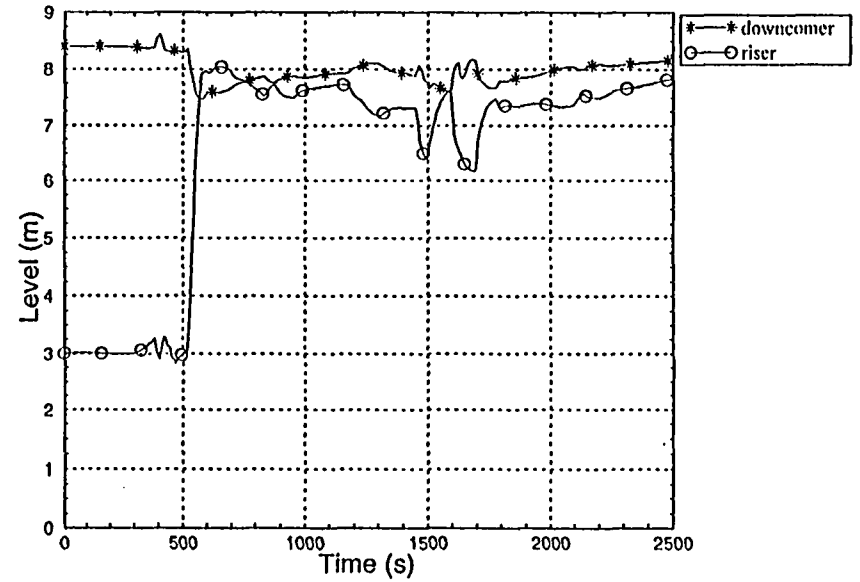


Figure 6.25.- Flow Regimes in SG Riser (Part 1)

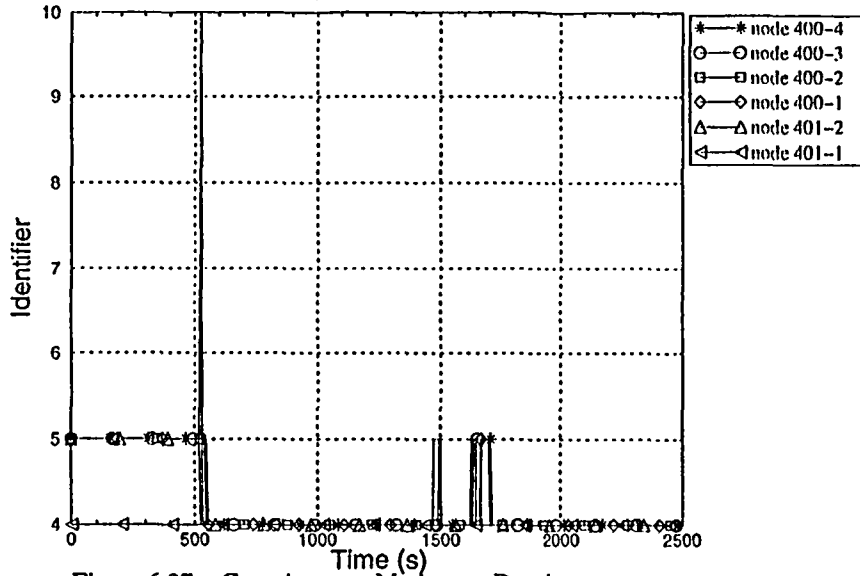


Figure 6.26.- Flow Regime in SG Riser (Part 2)

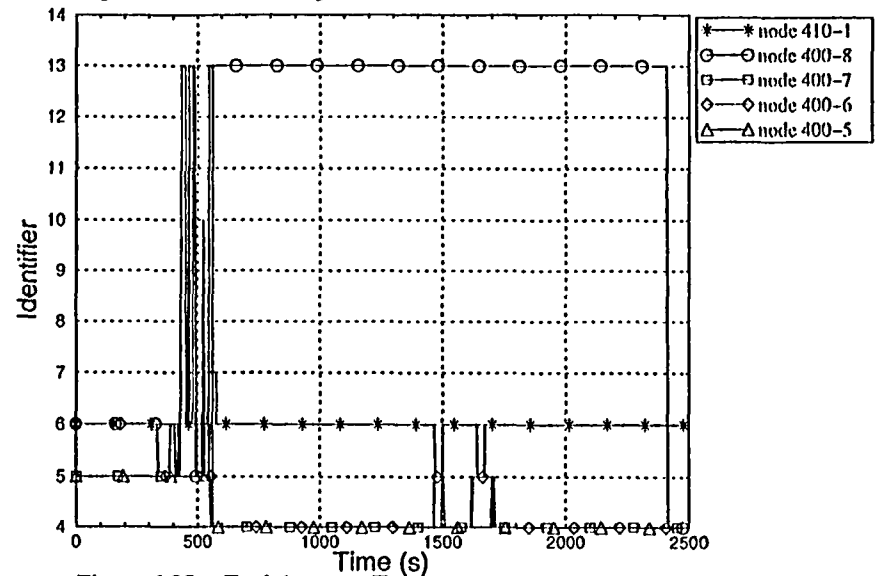


Figure 6.27.- Core Average Moderator Density

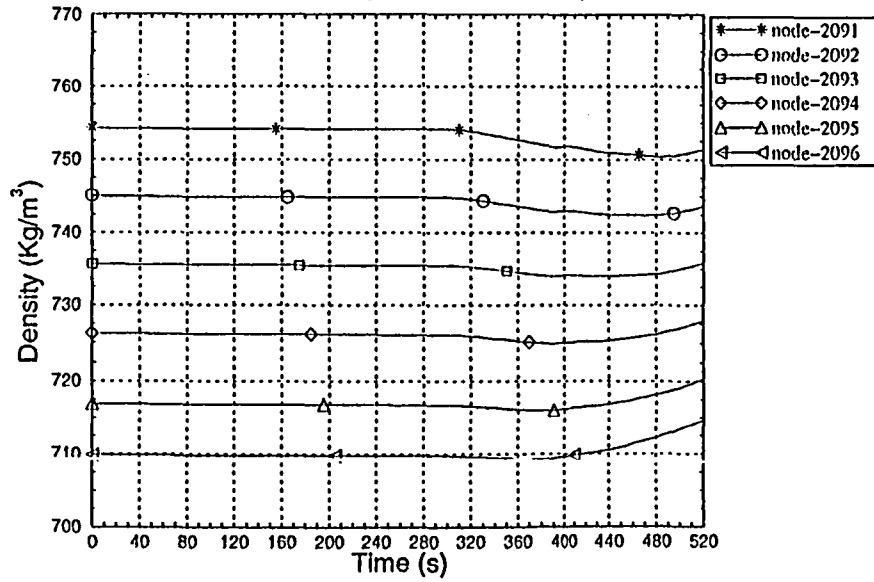


Figure 6.28.- Fuel Average Temperature

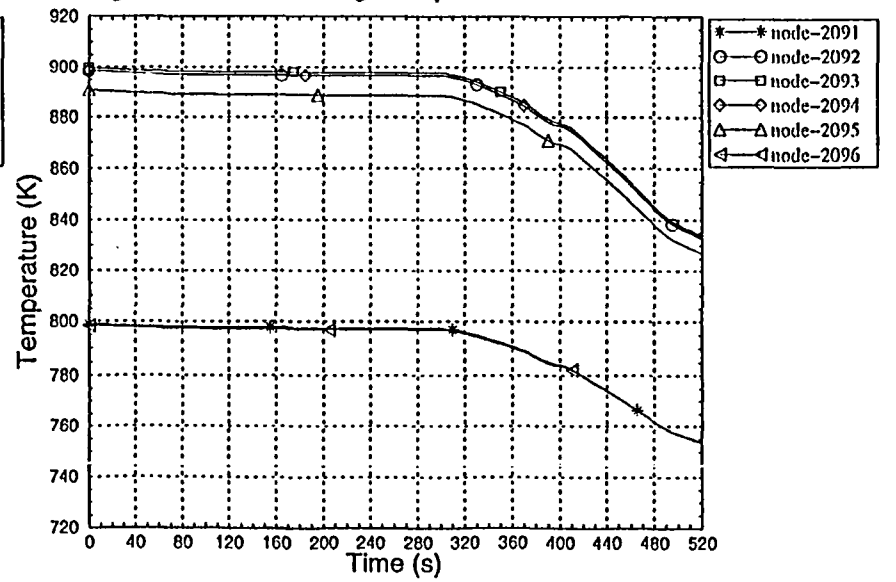


Figure 6.29.- Pressurizer Wall Steam Generation

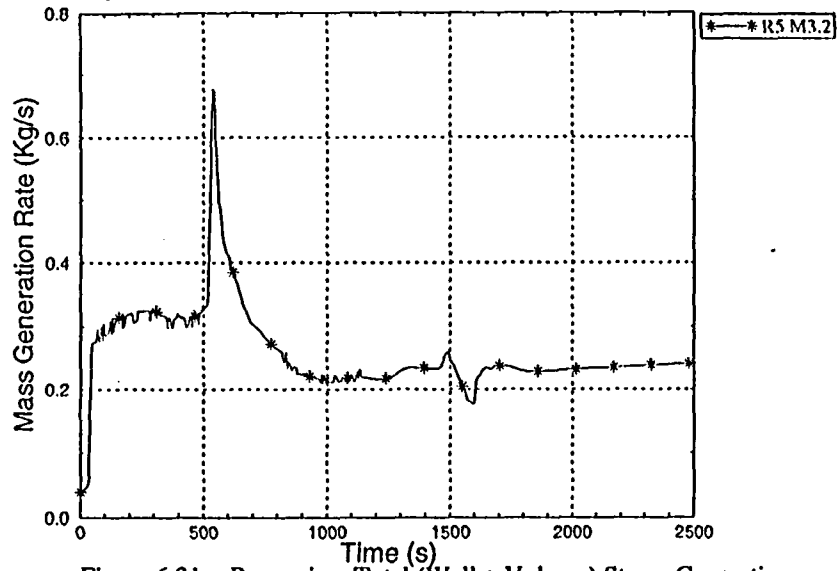


Figure 6.30.- Pressurizer Volume Steam Generation

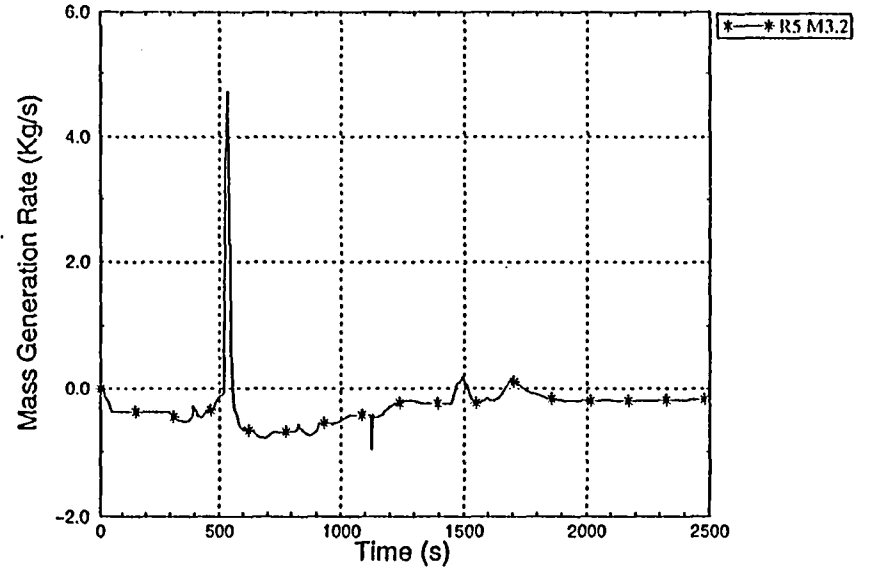
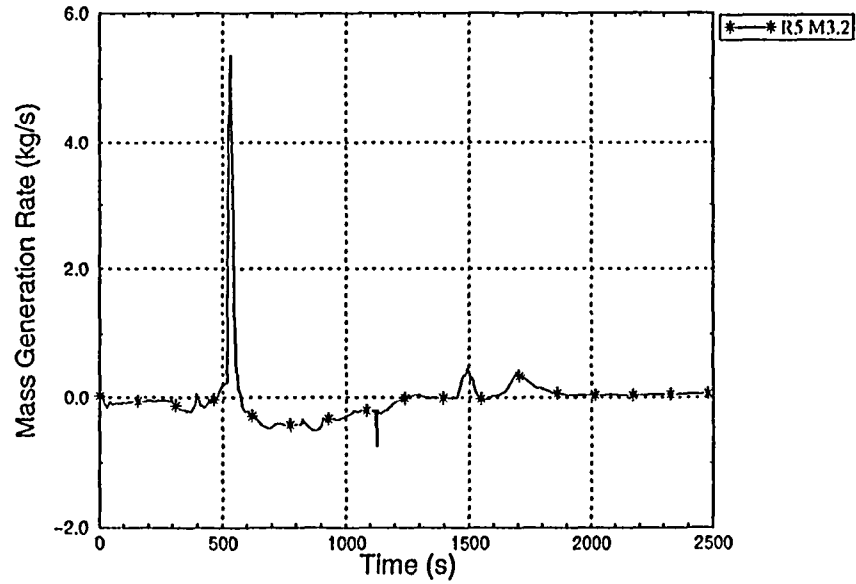


Figure 6.31.- Pressurizer Total (Wall + Volume) Steam Generation



7. SENSITIVITY CALCULATIONS

A set of sensitivity calculations have been carried out trying to identify the importance of some factors on the calculated plant response. The analysis presented in the following subsections cover the sensitivity of both PZR response to model options and nodalization and SG level response to coded flow regime transitions.

7.1. Flow Regime Transitions

As was said in Section 6.2.7, the SG level abnormal behaviour during the turbine load reduction phase of the transient, gave rise to a sensitivity calculation on coded flow regime transitions. The aim of this calculation was to smooth the transition between slug and annular-mist regimes. This was accomplished by increasing the size of the transition region, from the "as coded" value of $\Delta\alpha_g=0.05$ to a value of 0.2. The expressions of variables "alphde" and "fanm" in subroutines PHANTJ and PHANTV were modified in that way.

As can be seen in figure 7.1 the modified code does not show the unrealistic level peak from the base case and compares well with plant data. The same can be said about the feedwater flow (Figure 7.2).

Therefore, it can be concluded that flow regime transitions should be smoothed or, which is the same, the calculated value of both interphase friction and heat transfer coefficients may need to be reviewed.

7.2. Level Tracking Option in PZR

This model option was checked in the pressurizer nodes. Surprisingly, the obtained results were worse than without activating it.

Figure 7.3 shows the calculated pressurizer pressure compared to both base case and plant data. This pressure experience an abnormal increase when the PZR level reach the node where the spray junction is located (Figures 4.1 and 6.2). This fact is due to oscillations in the condensation rate within the pressurizer (Figures 7.4 and 7.5),

particularly in the node cited above where the condensation is almost suppressed.

This kind of behaviour was also found in MOD2.5 version calculations, as will be shown in Section 8.

Therefore, it could be recommended that care should be taken when using the level tracking option.

7.3. Pressurizer Pressure Response

As was said in Sections 6.2.3 and scarcely along 6.2.4 to 6.2.8, the pressurizer pressure (Figure 6.1) was matched to plant data by imposing a spray flow rate (Figures 6.14 and 6.15) higher than design data. In order to identify the origin of that discrepancy a series of three sensitivity calculations were carried out.

All of these calculations have a constant spray valve opening during the whole transient, this is the one necessary to match the depressurization rate before the reactor trip. So, all of them give the same spray flow (Figure 7.7).

The first calculation quoted "R5 M3.2 rcte" is the base case with a constant spray valve opening. The second one quoted "R5 M3.2 nod" has, in addition to the first, a finer nodalization of both pressurizer and spray line. And the third one quoted "R5 M3.2 kSS", in addition to the two above, has been built a decreased pressurizer wall thermal conductivity, from $46 \text{ W/m}^2\cdot\text{K}$ (carbon steel) to $16 \text{ W/m}^2\cdot\text{K}$ (stainless steel). The actual composition of pressurizer wall is carbon steel with a stainless steel liner, so this case is supposed to bound the actual one.

Figure 7.6 shows the obtained results in comparison with plant data. As can be observed a finer nodalization does not substantially affect the calculation. A modified wall conductivity offers better results for the minimum pressure reached just after the reactor trip, but at long term the pressure approaches the other calculations.

In fact, a less wall conductivity only slows down the heat transfer from the wall inside. This gives a less wall evaporation peak (Figure 7.8) at the beginning but a greater

value from that moment on.

Therefore, it was concluded that the reason for a pressure evolution constantly greater than plant data, with the spray valve fully opened and giving a mass flow rate similar to that of design data, should be other than nodalization or wall thermal properties. As was quoted above, an specialized model for spray could be a better solution, due to the better efficiency of the spray when PZR level is lower. This fact would justify the higher flow required to match the pressure evolution after the reactor trip.

It was decided to run one more sensitivity calculation on the average temperature uncertainty, as it is explained in the next section, because it is the only remaining cause that would have a major contribution right after reactor trip.

7.4. Average Temperature Uncertainty

As was said along Section 6.2 and after the above series of sensitivity calculations, there was a suspect of a large uncertainty on the average temperature measurement based on the following reasons: first, the lack of coherence between SG pressure and average temperature, second, the superimposing of a spray valve flow to match the PZR pressure plant data, and finally that the calculated minimum PZR level after the reactor trip is a 5% greater than registered one.

Therefore, a sensitivity calculation was designed with the following restrictions: a) the steam-dump flow would be as needed to match SG pressure plant data, b) it is assumed that the registered average temperature was near 3K above the real average one, c) the spray valve opening is maintained during the whole calculation.

The second assumption is supported by the existence of streaming effects, which are of relevance due to sensors location, and by the data channel selection logic employed in plant, which always selects the maximum of three independent channels /9/. These factors appears to be magnified when the temperature jump across the SG tubes is low (Figure 6.17). At least for this transient, the coherence between SG pressure and average temperature is almost recovered after the RCP trip, when the ΔT returns to be high.

Figures 7.9 to 7.12 show the results of this analysis. The data with a 3K shift in average temperature have the word “tav” in their legend. As may be observed, it is possible to match at the same time the SG pressure and the registered average temperature. With regard to the PZR pressure, the effect of a lower temperature of the PZR inflow from the surge line, even important, is not enough to get the correct pressure evolution between reactor trip and pump trip.

Therefore, the remaining deviation between calculated and registered pressure evolution could be attributed either to RELAP5 condensation models (more specifically, the condensation due to spray flows) or to transient timing uncertainties, or both. Further studies are in course to assess the effect of a detailed spray simulation, and the possibility of coupling these calculations to RELAP5.

The observed discrepancy in the PZR level evolution, can be explained by introducing a correction due to level calibration. This correction would give an actual level (as calculated) less than the measured one at pressures less than the nominal one. The magnitude of the correction depends on the level, and would be near 7% for the maximum level reached during the present transient, which compares well with the calculated one (Figure 7.12).

Figure 7.1.- Sensitivity to smooth regime transition: SG Level

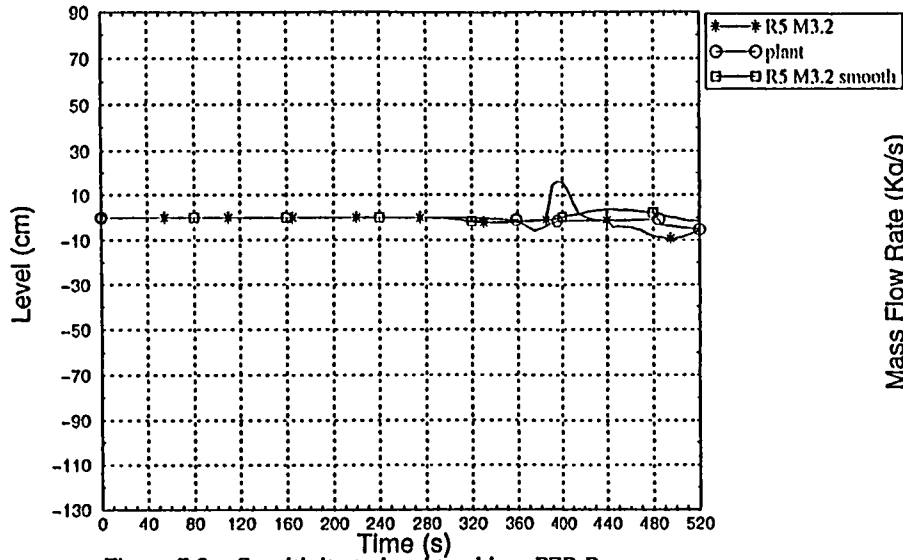


Figure 7.2.- Sensitivity to smooth regime transition: MFW Flow

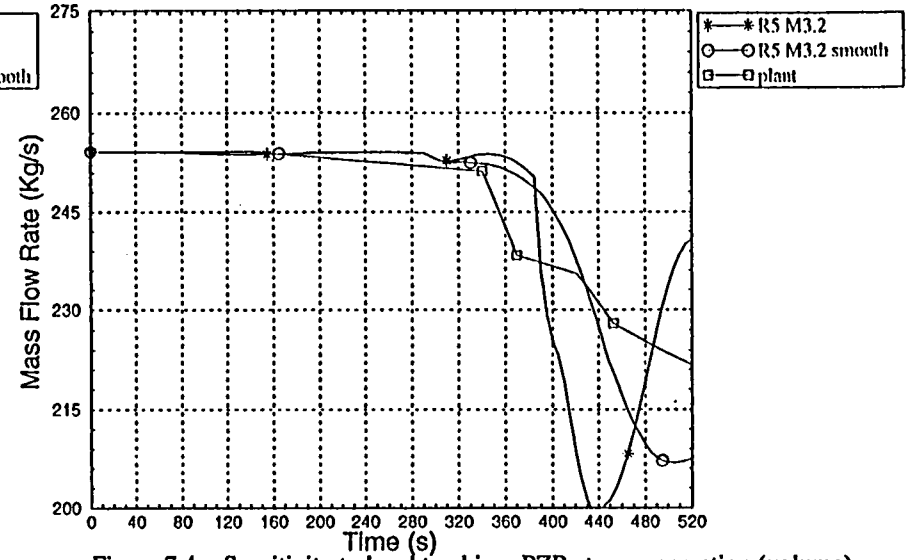


Figure 7.3.- Sensitivity to level tracking: PZR Pressure

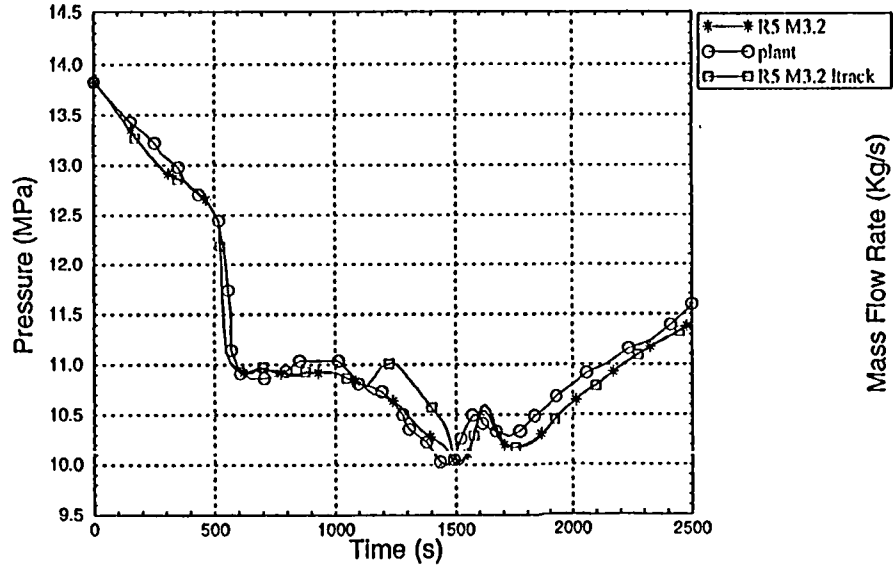


Figure 7.4.- Sensitivity to level tracking: PZR steam generation (volume)

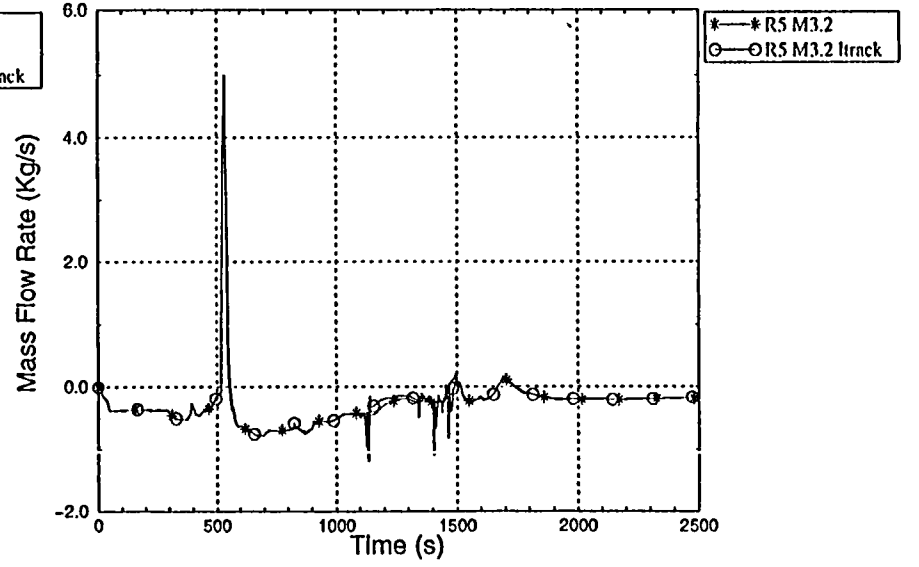


Figure 7.5.— Sensitivity to level tracking: PZR steam generation (wall)

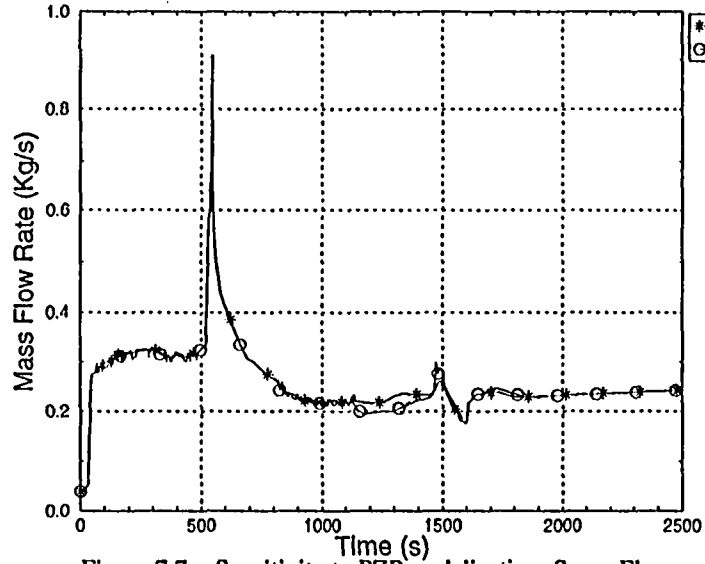


Figure 7.6.— Sensitivity to PZR nodalization: PZR Pressure

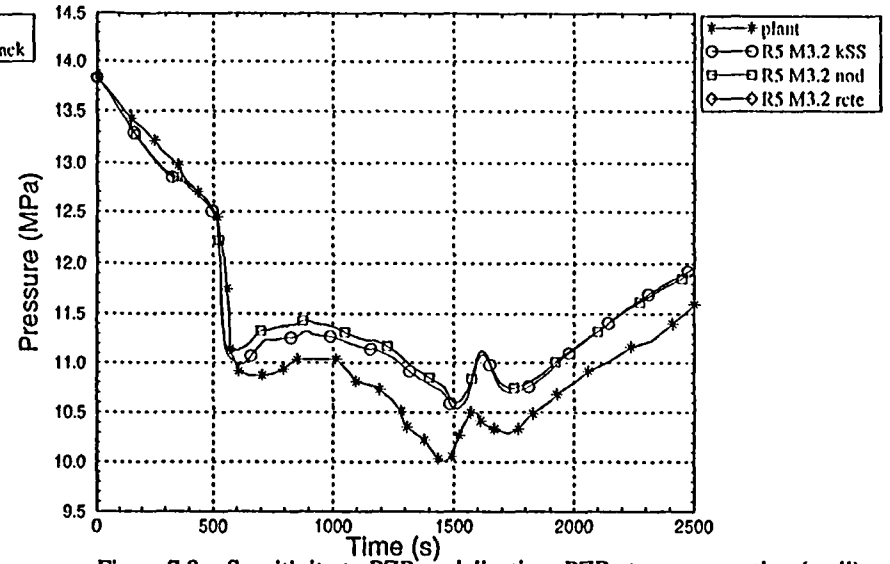


Figure 7.7.— Sensitivity to PZR nodalization: Spray Flow

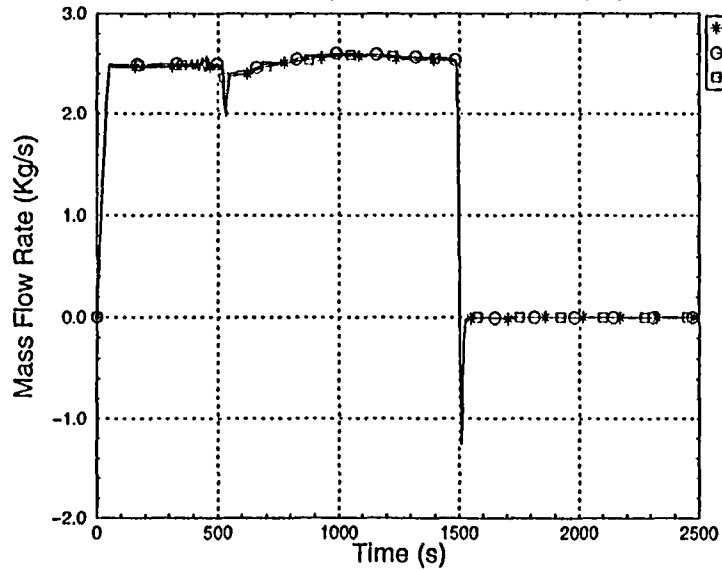


Figure 7.8.— Sensitivity to PZR nodalization: PZR steam generation (wall)

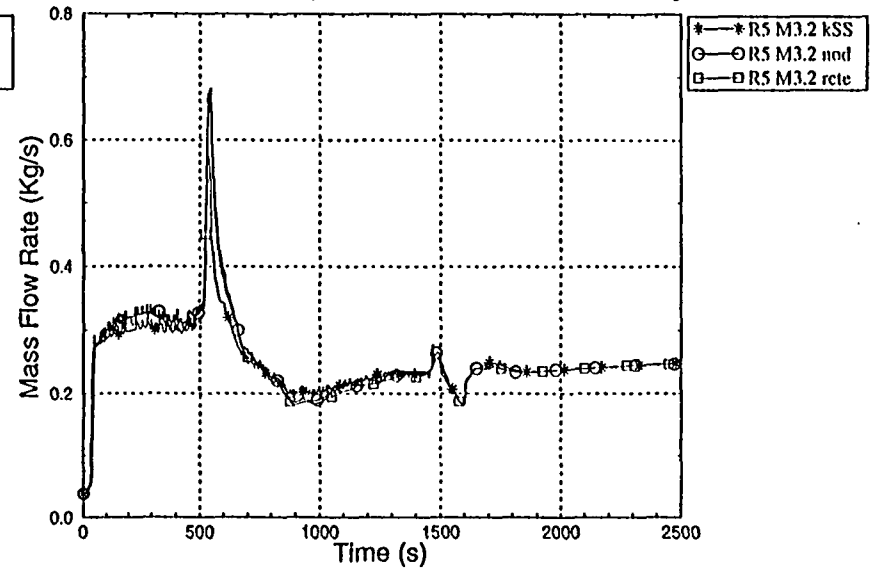


Figure 7.9.- Sensitivity to Tav_g uncertainty: PZR pressure

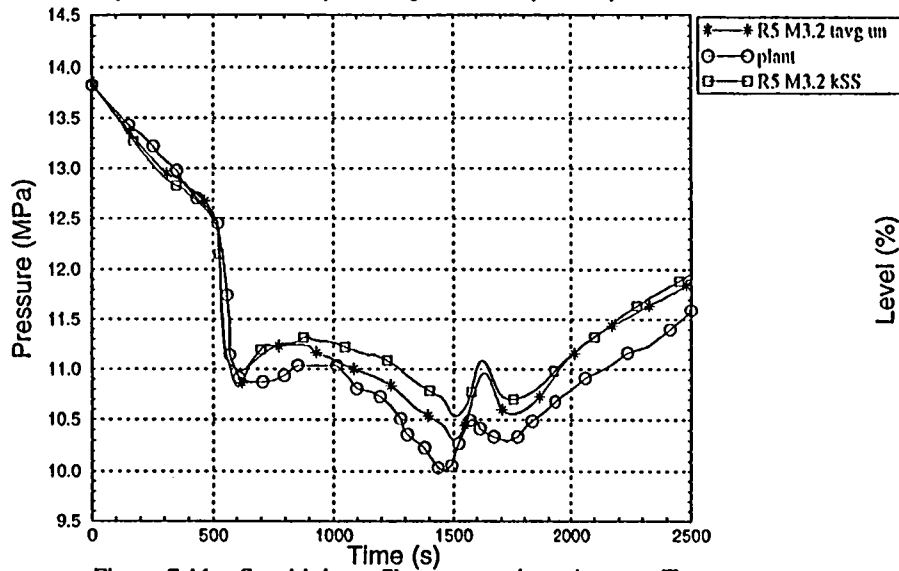


Figure 7.10.- Sensitivity to Tav_g uncertainty: PZR level

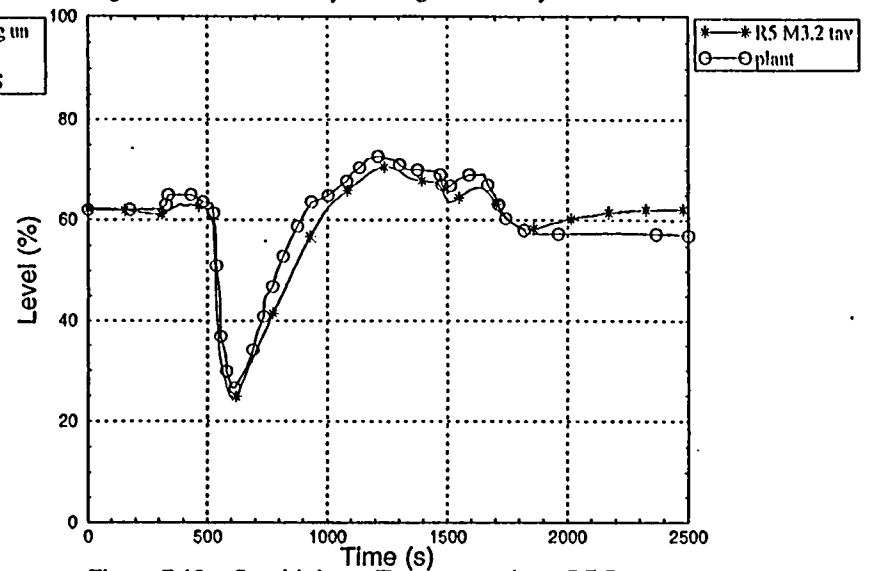


Figure 7.11.- Sensitivity to Tav_g uncertainty: Average Temperature

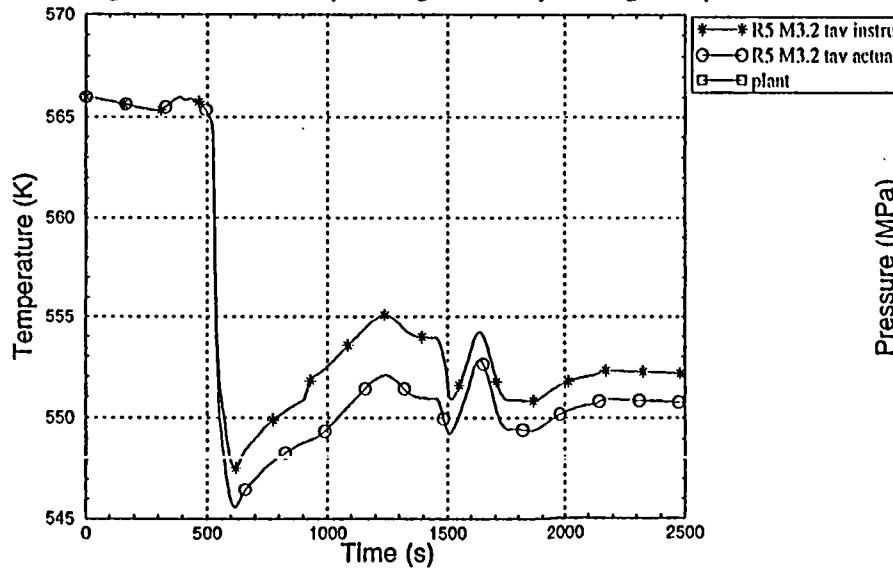
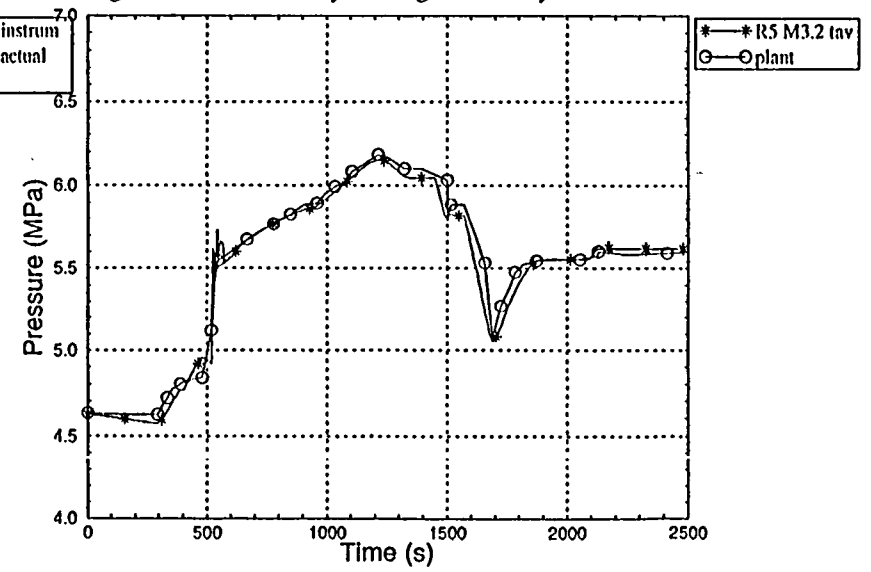


Figure 7.12.- Sensitivity to Tav_g uncertainty: SG Pressure



8. RELAP5/MOD3.2 - MOD2.5 COMPARISON

This section presents a comparison between the MOD3.2 and MOD2.5 versions of RELAP5. The aim of the analysis is to show major differences between both versions when applying to the same transient.

The input deck for MOD2.5 is basically the same as that for MOD3.2 with only the following modifications:

- 1) heat structure cards series lcccn801 and lcccn901 were modified to take into account format differences
- 2) heat structures with boundary condition 110 (vertical bundle), this is the core and secondary side of steam generator tubes, were returned to 1 (default),
- 3) new volume control flags (i.e. bundle) were eliminated,
- 4) new junction control flags (i.e. CCFL) were eliminated,
- 5) junction diameter and CCFL data cards were eliminated.

The nominal steam generator pressure in steady-state conditions, was achieved by only modifying the secondary heat transfer hydraulic diameter within the heat structures representing the SG tubes. Table 8.1 shows a comparison of steady-state results between MOD2.5 and MOD3.2, the table only gathers major differences.

Parameter	Plant data	MOD3.2	MOD2.5
ΔT (K)	24.2 / 23 (*)	24.3	24.9
RCS Mass Flow Rate (Kg/s)	3780	3769	3670 (**)
SG Circulation Ratio (-) (***)	2.04	2.035	2.16
SG Secondary Water Mass (% of vendor's nominal)	-	100	89

(*) The best-estimate value is 24.2K, and the registered one is 23K. The mismatch between these values is due to thermal streaming phenomena in hot and cross-over legs, and to measurement error as well.

(**) Obtained with the same input for RCS pressure losses

(***) Circulation ratio = $\dot{m}_{\text{downcomer}} / \dot{m}_{\text{vapor}}$

Table 8.1. MOD3.2 / MOD2.5 comparison: Steady-state results.

It is evident that the major difference between both versions is the secondary water mass, which is 11% less than vendor's nominal for MOD2.5. As was said in Section 5.2.1 the void fraction profile in the SG riser calculated by MOD3.2 is responsible of an accumulation of liquid water in the upper nodes of the riser. This void profile is not increasing uniformly with height as in MOD2.5. The problem was traced to the interphase friction factor which greatly differs from one flow regime to another.

The PZR pressure calculated by MOD2.5 (Figure 8.1) exhibits an abnormal behaviour when the level (Figure 8.2) reaches the node where the spray junction is located. The reason for this behaviour are oscillations in the condensation rate (Figure 8.7 and 8.8) within that PZR node. The same was found when checking the level tracking option in MOD3.2 (see Section 7.2).

Therefore, with respect to condensation/evaporation phenomena within the pressurizer, one can conclude that MOD3.2 models have improved its predictions. Moreover, taking into account the results obtained from the sensitivity calculations presented in Sections 7.3 and 7.4, one can conclude that, for MOD3.2, a finer PZR nodalization is not necessary to get good predictions.

The steam generator pressure peak just after the reactor trip (Figure 8.4) is near 2 bar greater than plant data and 2.7 bar greater than MOD3.2. This means that, in spite of a lower secondary water mass, the primary to secondary heat transfer is overestimated by MOD2.5 correlations, at least after the reactor trip when the circulation loop within the steam generator is broken. This fact is also reflected in the minimum average temperature reached just after the reactor trip, which is lower in MOD2.5 (Figure 8.3).

Looking to the steam generator level evolution before the reactor trip (Figures 8.5 and 8.6), it can be seen that MOD2.5 does not show the unrealistic peak showed by MOD3.2, and that its behaviour is similar to the *ad hoc* smoothed version of MOD3.2 (Figure 7.1). So, one can conclude the same than in Section 7.1: in MOD3.2, flow regime transitions should be smoothed or, which is the same, the calculated value of both interphase friction and heat transfer coefficients may need to be reviewed.

As an overall conclusion, the MOD3.2 version has shown clear improvements in

comparison with MOD2.5, on the treatment of condensation/evaporation phenomena within the PZR and on the prediction of primary to secondary heat transfer rates. On the contrary, MOD3.2 has also shown some unphysical results related to flow regime transitions which does not appear in MOD2.5. The lack of modelling drop fields, as in sprays, appears to be a shortcoming that should be implemented in future versions of the code.

Figure 8.1.- RELAP5 Mod3.2 / Mod2.5 Comparison: PZR Pressure

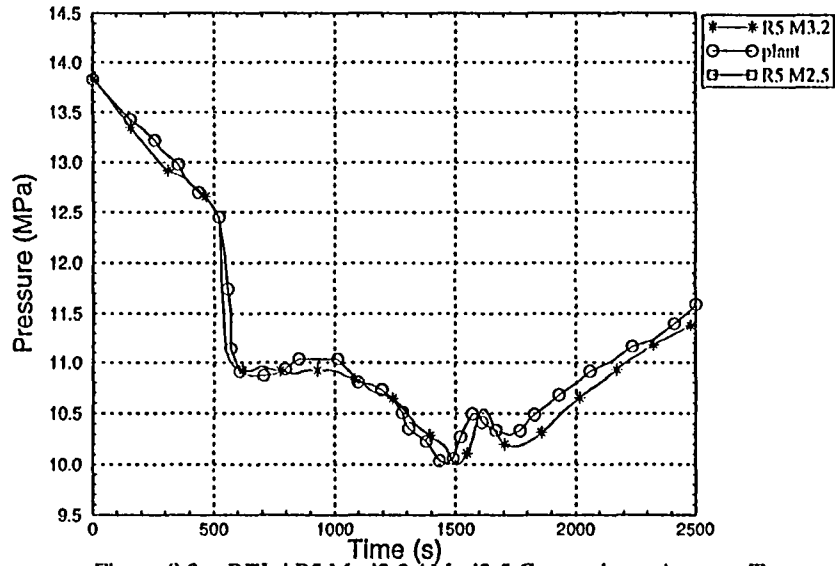


Figure 8.2.- RELAP5 Mod3.2 / Mod2.5 Comparison: PZR Level

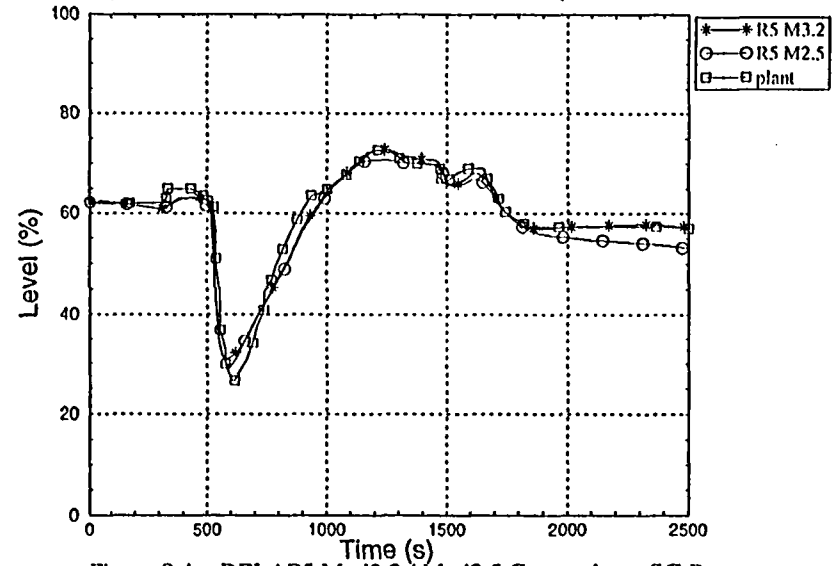


Figure 8.3.- RELAP5 Mod3.2 / Mod2.5 Comparison: Average Temperature

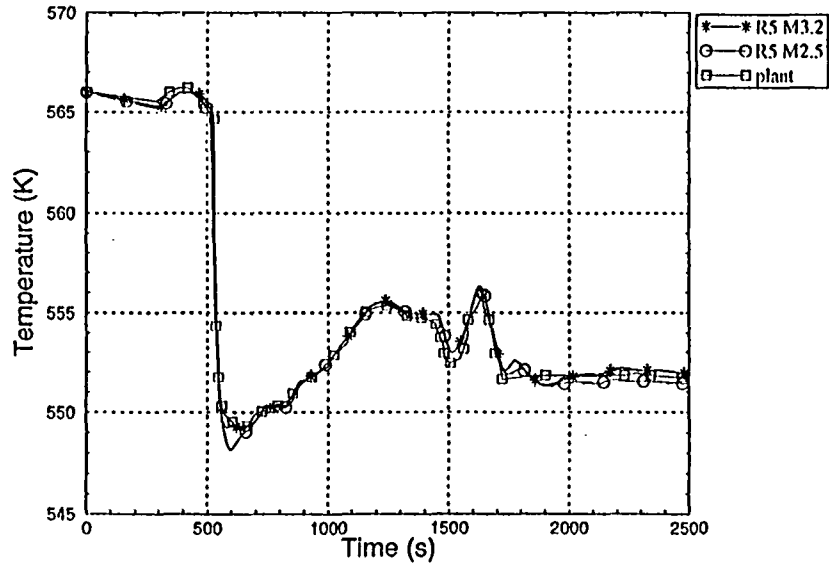


Figure 8.4.- RELAP5 Mod3.2 / Mod2.5 Comparison: SG Pressure

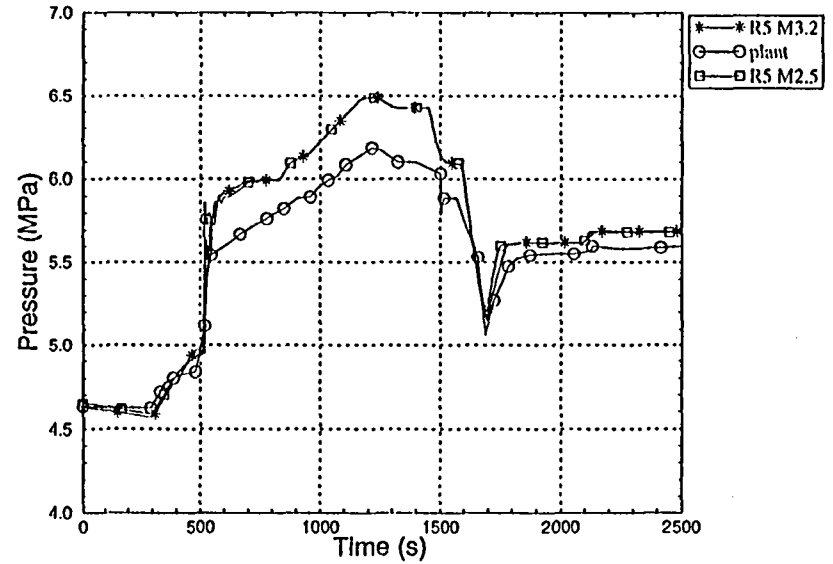


Figure 8.5.- RELAP5 Mod3.2 / Mod2.5 Comparison: SG Level

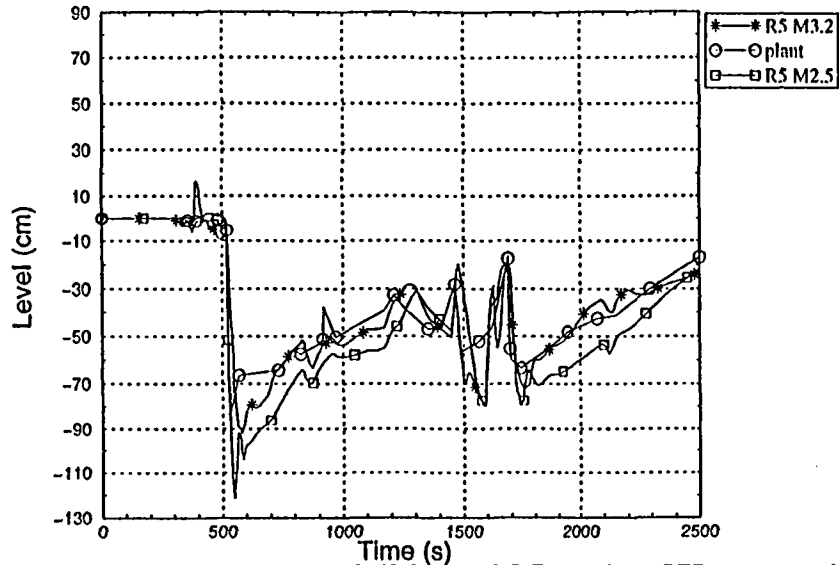


Figure 8.6.- RELAP5 Mod3.2/Mod2.5 Comparison:SG Level (0-600s)

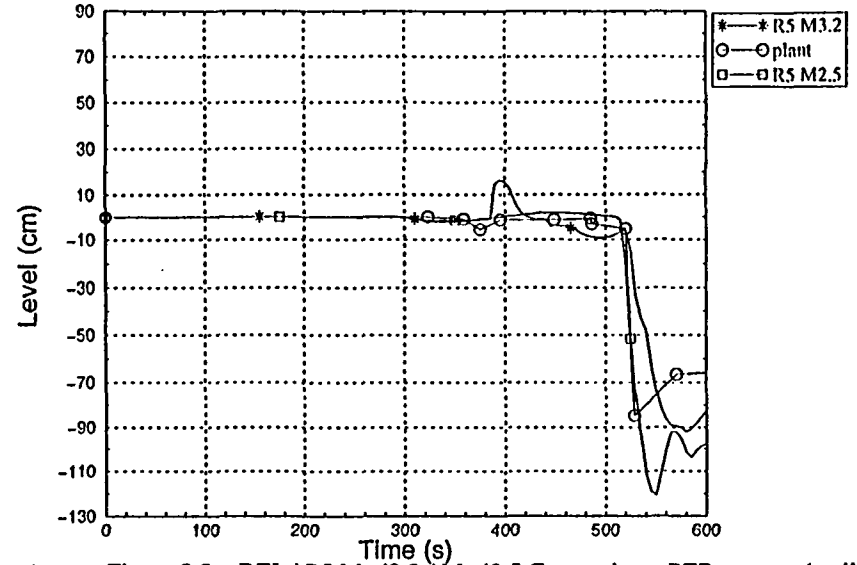


Figure 8.7.- RELAP5 Mod3.2 / Mod2.5 Comparison: PZR vapgen (volume)

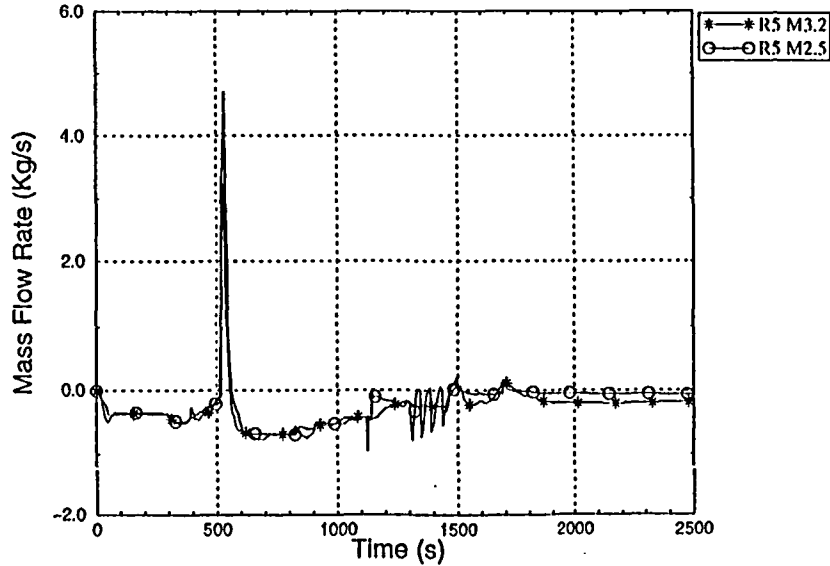
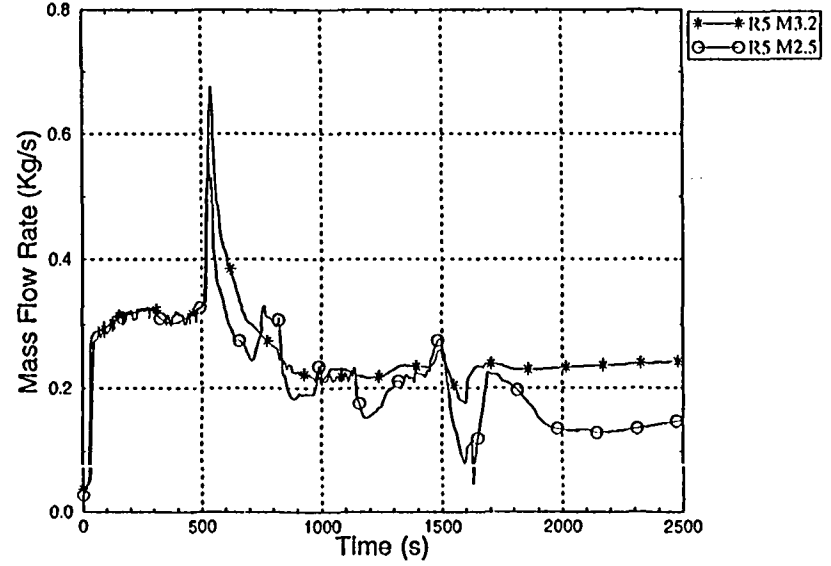


Figure 8.8.- RELAP5 Mod3.2 / Mod2.5 Comparison: PZR vapgen (wall)



9. CONCLUSIONS

The time duration of the analyzed transient and the variety of events and phenomena implied, which include depressurization by spray, load reduction and reactor kinetics, reactor and turbine trips, and natural circulation, have been very useful to check both plant model fitness and RELAP5/MOD3.2 performance.

In spite of the difficulties encountered during the analysis, caused mainly by plant data uncertainties, a coherent and quite accurate description of the evolution of plant conditions has been obtained, in which sensitivity calculations have played an important role.

RELAP5 calculations have helped in deducing, confirming or solving many of plant data uncertainties. On its own part, plant data have helped to gain some insights about code behaviour, enhancements and shortcomings.

In general, the José Cabrera plant model for RELAP5/MOD3.2, and the code itself, reproduce adequately, with some few exceptions explained below, both plant and control system behaviour and the different thermalhydraulic phenomena along the present transient. As the majority of operational transient include some or all of the events in the analyzed one, the good results obtained with the plant model support a wide range of applications like, among others, development and checking of "Emergency Operational Procedures", plant design review, or safety analysis.

The simulation of the present transient is, within the identified uncertainties, quite satisfactory because it has been possible to determine the sequence of events, phenomena and control system actuation, which explain the registered plant behaviour.

The comparison, between calculated variables and plant data, taking also into account sensitivity calculations, has shown a good agreement with regard to both steady-state and transient values, that is, maximum, minimum, slope and stationary values. Nevertheless, in a few exceptions some discrepancies were not completely solved and were assigned to more than one reason.

The following paragraphs summarize some useful conclusions, not only for the model but also for RELAP5/MOD3.2 code, which can be concluded from the analysis.

- 1) The steady-state secondary water mass from MOD3.2 is near the vendor's nominal value. This extra mass is accumulated in the upper nodes of the riser. The new interphase friction factor and heat transfer coefficient correlations incorporated in MOD3.2 were identified as responsible of this fact.

This extra mass can be misdistributed, as is partly indicated by the SG level evolution just after the reactor trip. This evolution was matched by imposing a lower closure time for the MFW isolation valve, so introducing less water in the steam generator. Nevertheless, abrupt flow regime transitions, which are responsible of large variations in the head exerted by the riser, mask any conclusion about the connection between the secondary water mass and level evolution after the trip.

- 2) As was demonstrated in a sensitivity calculation with a modified RELAP5/MOD3.2 code, the smoothing of slug to annular-mist transition suppress unphysical steam generator level behaviour during the load reduction phase of the transient. So, it is considered important to review this transition or, which is nearly the same, to review the calculated magnitude of interphase friction and heat transfer coefficients.
- 3) It is believed that condensation phenomena is underestimated by RELAP5/MOD3.2, specially for geometries implying spray, like the pressurizer or steam generator volume below the feedwater ring. Several sensitivity studies have been carried out to estimate the effect of the uncertainties in related variables, and it has been shown that they failed to provide a satisfactory answer to the differences observed between plant registers and simulation. These differences have been well correlated with the effect of varying the PZR level in the spray efficiency. Further studies are in course to assess the effect of a detailed simulation of the spray in condensation and pressure transient evolution.
- 4) The level tracking option was checked within the pressurizer nodes obtaining worse results, similar to those obtained with MOD2.5. When the PZR level reaches the

node where the spray junction is located, the condensation within that node becomes unstable or even suppressed, so the pressure experience an increase.

This problem does not appear in MOD3.2 without level tracking, which represents a clear improvement with respect to MOD2.5 models. Care should be taken when using this option.

- 5) Sensitivity calculations have shown the importance of correctly modeling the thermal properties of the pressurizer wall, to predict the minimum pressure after a rapid depressurization.
- 6) Pressure losses due to wall friction are, in MOD3.2, lower than in MOD2.5, giving for the same values of rugosity a primary system flow 2% higher.
- 7) The streaming phenomena within the primary loop and the data selection logic for the average temperature signal (maximum of three channels), was identified as responsible of the lack of coherence between both calculated and registered steam generator pressure and average temperature. Assuming a difference of 3°C between actual and registered values of the average temperature, solves that problem.

As an overall conclusion, in spite of different shortcomings of the code, this transient study has shown the adequacy and accuracy of the actual RELAP5/MOD 3.2 José Cabrera NPP plant model for analyzing real plant transients, observing a clear improvement with respect to earlier versions of the code and the NPP model.

The particular behaviour of the spray valve in this transient has shown that the model implemented for MOD3.2 version do not succeed in simulate the pressure response in the plant, indicating a possible task for improving code capabilities.

10. REFERENCES

- /1/ "José Cabrera Nuclear Power Plant Final Safety Analysis Report", Revisión 8 (1995).
- /2/ J.Fornieles, UNION FENOSA, "Central Nuclear José Cabrera: Informe de disparo de la central por disparo del reactor (motivado por baja presión, causada por la apertura local de la PCV-400A)", (Trip Report) ID-95, Septiembre, 1984.
- /3/ V.H. Ransom & R.J. Wagner. "RELAP5/MOD2 Code Manual", NUREG/CR-4312, EGG-2396, INEL, USA, December, 1985.
- /4/ "RELAP5/MOD3 Code Manual", INEL-95/0174, NUREG/CR-5535, June 1995.
- /5/ R.Arroyo, L.Rebollo, "Assessment of RELAP5/MOD2 Against a Pressurizer Spray Valve Inadverted Fully Opening Transient and Recovery by Natural Circulation in José Cabrera Nuclear Station", NUREG/IA-0124, ICSP-JC-SPR-R, June, 1993.
- /6/ Unión Eléctrica Fenosa, "Modelo de C.N. José Cabrera para el código RELAP5/MOD2", Revisión 2, 1996.
- /7/ J.G.Pindado, E. Moralo, "Actualización del Modelo de Planta de la Central Nuclear José Cabrera para el Código RELAP5/MOD3", UFISA-PMSA, Rev.1, Febrero 1997.
- /8/ J.G.Pindado, P.Moreno, J.Blanco, "Validación del Modelo de Planta de la Central Nuclear José Cabrera para el Código RELAP", UFISA-PMSA, Diciembre 1995.
- /9/ Blondiaux et al, "Central Nuclear Jose Cabrera Reactor Coolant System Temperatures", WENX 96/14, Westinghouse, May 1996.

BIBLIOGRAPHIC DATA SHEET

(See instructions on the reverse)

1. REPORT NUMBER
(Assigned by NRC, Add Vol., Supp., Rev.,
and Addendum Numbers, if any.)

NUREG/IA-0194

2. TITLE AND SUBTITLE

Analysis of Inadvertent Pressurizer Spray Valve Opening
Real Transient with RELAP5/MOD3.2

3. DATE REPORT PUBLISHED

MONTH	YEAR
January	2001

4. FIN OR GRANT NUMBER

5. AUTHOR(S)

J. Blanco, L. Rebollo, E. Moralo, J. Pindado, P. Moreno

6. TYPE OF REPORT

Technical

7. PERIOD COVERED *(Inclusive Dates)*

8. PERFORMING ORGANIZATION - NAME AND ADDRESS *(If NRC, provide Division, Office or Region, U.S. Nuclear Regulatory Commission, and mailing address; if contractor, provide name and mailing address.)*

UNESA
C/ Francisco Gervas No. 3
28020 Madrid
SPAIN

9. SPONSORING ORGANIZATION - NAME AND ADDRESS *(If NRC, type "Same as above"; if contractor, provide NRC Division, Office or Region, U.S. Nuclear Regulatory Commission, and mailing address.)*

Division of Systems Analysis and Regulatory Effectiveness
Office of Nuclear Regulatory Research
U.S. Nuclear Regulatory Commission
Washington, DC 20555-0001

10. SUPPLEMENTARY NOTES

11. ABSTRACT *(200 words or less)*

This document presents the comparison between the simulation results and the plant measurements of an actual event that took place in Jose Cabrera Nuclear Power Plant (NPP) in August 30, 1984. The event was originated by a continuous and inadvertent opening of the pressurizer spray valve. Jose Cabrera NPP is a 510 Mwth single loop Westinghouse PWR owned by UNION ELECTRICA FENOSA, S.A (UNION FENOSA) a Spanish utility that participates in the Code Application and Maintenance Project (CAMP) as a member of UNIDAD ELECTRICA, S.A. (UNESA). The simulation has been carried out with the RELAP5/MOD3.2 code, running on a Digital AlphaServer 2000 4/200 computer under DIGITAL-UNIX operating system. The main phenomena of the transient have been calculated correctly and some conclusions about the performance of new models and correlations incorporated in the MOD3.2 version, have been obtained. Several considerations about spray modeling in RELAP5/MOD3.2 are given. Additionally, a comparison with the MOD2.5 version results has shown some improvements and shortcomings of the new version.

12. KEY WORDS/DESCRIPTORS *(List words or phrases that will assist researchers in locating the report.)*

Pressurizer Spray Valve
RELAP5/MOD3.2

13. AVAILABILITY STATEMENT

unlimited

14. SECURITY CLASSIFICATION

(This Page)

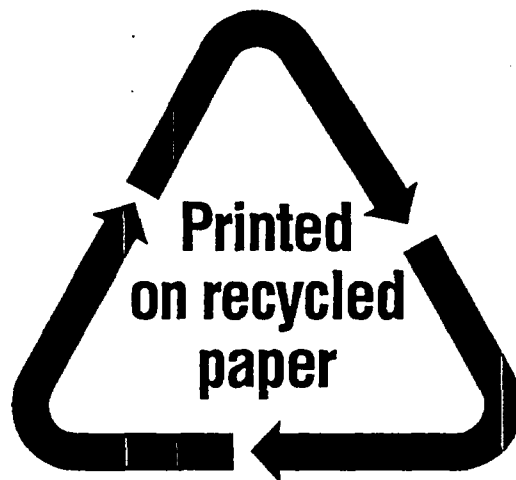
unclassified

(This Report)

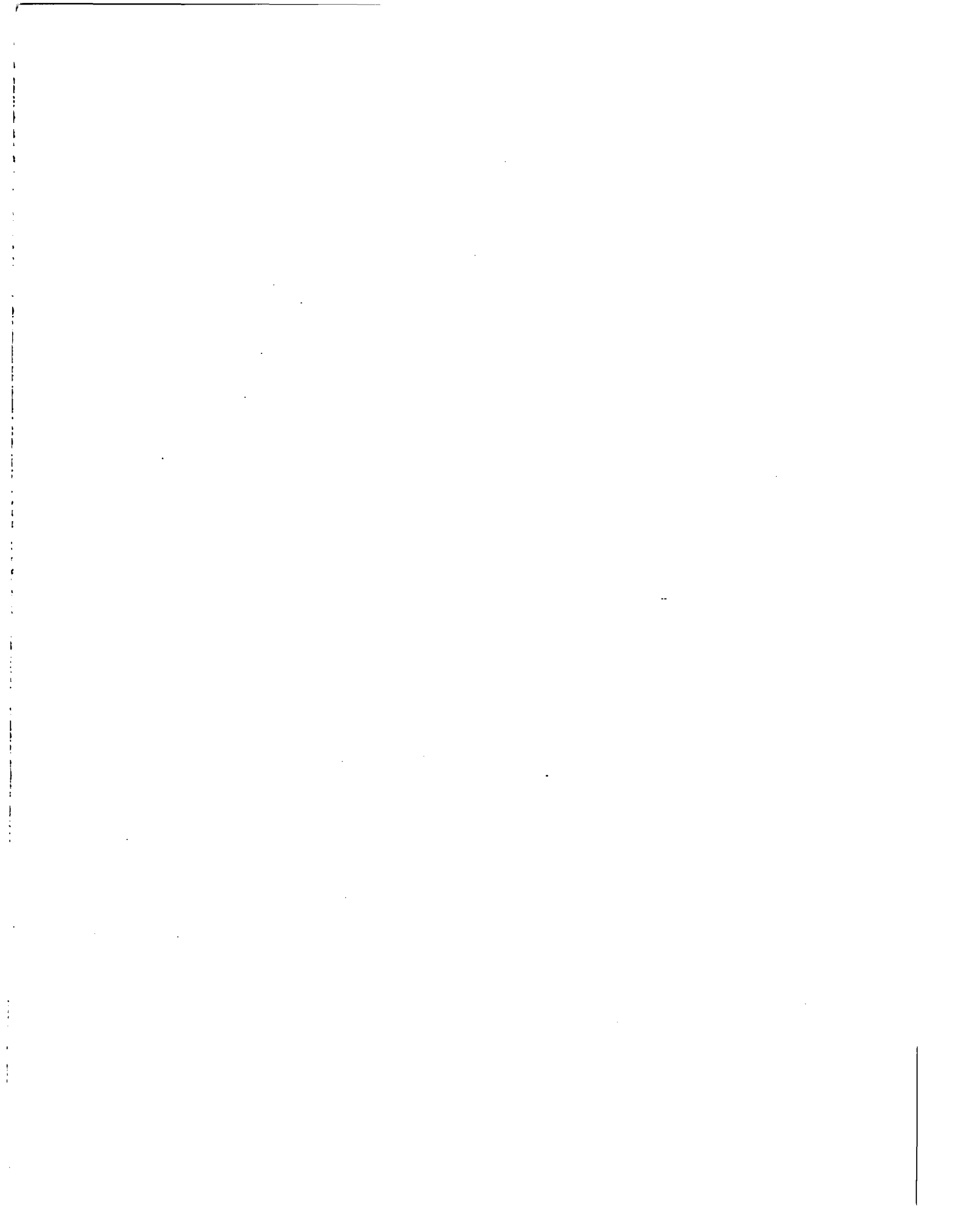
unclassified

15. NUMBER OF PAGES

16. PRICE



Federal Recycling Program



UNITED STATES
NUCLEAR REGULATORY COMMISSION
WASHINGTON, DC 20555-0001

OFFICIAL BUSINESS
PENALTY FOR PRIVATE USE, \$300